Ab initio Study of the Diatomic Fluorides FeF, CoF, NiF, and CuF

Constantine Koukounas and Aristides Mavridis*

Laboratory of Physical Chemistry, Department of Chemistry, National and Kapodistrian University of Athens, P.O. Box 64 004, 15710 Zografou, Athens, Greece

Received: June 8, 2008; Revised Manuscript Received: July 31, 2008

The late-3d transition-metal diatomic fluorides MF = FeF, CoF, NiF, and CuF have been studied using variational multireference (MRCI) and coupled-cluster [RCCSD(T)] methods, combined with large to very large basis sets. We examined a total of 35 $^{2S+1}|\Lambda|$ states, constructing as well 29 full potential energy curves through the MRCI method. All examined states are ionic, diabatically correlating to $M^+ + F^-(^1S)$. Notwithstanding the "eccentric" character of the 3d transition metals and the difficulties to accurately be described with all-electron ab initio methods, our results are, in general, in very good agreement with available experimental numbers.

1. Introduction

We have recently studied the electronic structure and bonding of the low-lying states of the neutral[1] and singly charged[2] 3d transition-metal monofluorides $ScF^{0,\pm1}$, $TiF^{0,\pm1}$, $VF^{0,\pm1}$, $CrF^{0,\pm1}$, and $MnF^{0,\pm1}$ through multireference variational and coupled-cluster (CC) methods. One of the conclusions of these works was the almost complete ionic character of both neutral and positively charged species as 0.7−0.8 e^- are transferred from the metal (or metal cation) to the fluorine atom. Therefore, the symmetries of molecular states seen as M^+F^- ($M^{2+}F^-$) are dictated by the symmetry of M^+ (M^{2+}) in the field of the spherical anion $F^-(^1S)$.[1,2]

Presently, we focus on the second half of the 3d transition-metal fluorides MF, M = Fe, Co, Ni, and Cu, thus concluding the monofluoride series of the first-row transition-metal elements. We remind at this point the importance of metal fluoride systems in the areas of applied sciences such as catalysis, high-temperature chemistry, surface chemistry, and astrophysics.[1,3]

The structure of the current paper mimics, more or less, that of refs 1 and 2. In section 2, the methods and basis sets are outlined, in section 3, certain relevant results on the metal atoms are given, while in the long section 4, subdivided into subsections 4A, 4B, 4C, and 4D, we discuss our results on FeF, CoF, NiF, and CuF, respectively. Finally, in section 5, we summarize our findings, and we outline an overall picture of the complete MF series, M = Sc−Cu.

2. Basis Sets and Methods

Two kinds of basis sets were used for the metal atoms, the ANO (averaged natural orbital) basis of Bauschlicher, 20s15p10d6f4g, of almost quadruple-ζ quality[4] and the newly developed extensive correlation-consistent basis sets of Balabanov and Peterson (BP), 28s20p12d4f3g2h1i, of quintuple cardinality.[5] For the fluorine atom, the augmented correlation-consistent basis sets of quadruple (AQZ) and quintuple (A5Z) cardinality of Dunning and co-workers were employed, that is, 13s7p4d3f2g and 15s9p5d4f3g2h, respectively.[6] The diffuse functions on the F atom were necessary to better describe the anionic character of the in situ F atom.[1] The ANO basis sets were combined with the AQZ and the BP with the A5Z of fluorine, both generally contracted to $[7s6p4d3f2g/_M6s5p4d3f2g/_F] \equiv 4Z$ and $[9s8p6d4f3g2h1i/_M7s6p5d4f3g2h/_F] \equiv 5Z$, comprising 164 and 280 spherical Gaussians, respectively. Finally, the largest basis set for the metals used in the present work is the BP one[5] augmented by a series of weighted core functions 2s+2p+2d+1f+1g+1h+1i, similarly contracted to $[11s10p8d5f4g3h2i] \equiv$ CBP and combined with the A5Z of the F atom. This basis set, tagged C5Z, contains 280 + 58 = 338 spherical Gaussians.

Our zeroth-order wave functions are of the complete active self-consistent field (CASSCF) valence type, defined by allotting the 4s3d electrons of the metal + the $2p_z$ electron of the F atom to the $4s3d4p_z(M) + 2p_z(F)$ orbitals, namely, 9, 10, and 11 e^- to 8 orbital functions for the FeF, CoF, and NiF molecules, respectively; see also refs 1 and 2. In the case of the CuF for the Σ^+ and Δ states (A_1 and A_1 or A_2 under C_{2v} constraints), the reference space was constructed by distributing 8 e^- [7 (Cu) + 1 (F)] to 9 orbitals, $[4s + 3d_{z^2} + 3d_{x^2-y^2} + 3d_{xy} + 4p_{x,y,z} + 5p_z + 2p_z(F)]$, in other words, keeping the $3d_{xz}$ and $3d_{yz}$ orbitals of Cu doubly occupied (inactive). For the Π states of CuF, 12 e^- were distributed to 10 orbital functions, 4s + 3d + 4p + $2p_z(F)$. This particular procedure was followed for technical reasons related to the idiosyncratic configuration of Cu($4s^13d^{10}$). In addition, in the Σ^+ and Δ states of CuF, we were forced to truncate the CASSCF reference space of the subsequent MRCI calculations by imposing a limit of 0.001 to the expansion coefficients of the CASSCF wave function.

Through single and double excitations out of the reference functions but including the full valence space of F(2s2p), the "dynamic" correlation was obtained. The size of the MRCI expansions were kept manageable by applying the internal contraction (ic) technique,[7] as implemented in the MOLPRO code.[8]

The coupled-cluster method RCCSD(T) (restricted coupled-cluster + singles + doubles + quasi-perturbative triples) was also applied for all accessible states to a single reference method of the MF species, M = Fe, Co, Ni, and Cu.[9]

Core-correlation effects were taken into consideration by including the $\sim 3s^23p^6$ semicore electrons of the metal atoms in the CI procedure, either at the MRCI or CC level, named C-MRCI and C-RCCSD(T). To give an idea of the size of the

* To whom correspondence should be addressed. E-mail: mavridis@chem.uoa.gr.

10.1021/jp805034w CCC: $40.75
Published on Web 10/09/2008

TABLE 1: Ionization Energies (eV) of Fe, Co, Ni, and Cu Calculated by Different Methods and Basis Sets

method[a]/basis set[b]	Fe	Co	Ni	Cu
MRCI/ANO	7.661	7.682	6.774	7.109
MRCI+Q	7.73	7.63	6.97	7.28
RCCSD(T)/ANO	7.712	7.530	7.166	7.442
MRCI/BP	7.668	7.645	6.735	7.097
MRCI+Q	7.73	7.59	6.94	7.27
RCCSD(T)/BP	7.723	7.495	7.127	7.437
C-MRCI+DKH2/CBP	7.710	8.101	7.336	7.206
C-MRCI+DKH2+Q	7.84	8.02	7.48	7.43
C-RCCSD(T)+DKH2/CBP	7.865	7.895	7.606	7.685
expt.[c]	7.902	7.881	7.640	7.7264

[a] In the MRCI calculations, the reference space contains six orbitals, one 4s + five 3d; therefore, for Cu, the MRCI reduces to CISD. [b] ANO = [7s6p4d3f2g], ref 4, BP = [9s8p6d4f3g2h1i], CBP = [11s10p8d5f4g3h2i], ref 5. [c] Ref 15b.

MRCI expansions, one of our largest C-MRCI calculations (FeF, $^4\Pi$), includes 2.4×10^9 configuration functions (CF), reduced to 18×10^6 at the icC-MRCI/C5Z approximation.

Scalar relativistic effects were taken into account by the second-order Douglas−Kroll−Hess (DKH2) approach.[10,11] In the DKH2 calculations, the basis sets of the metal atoms were recontracted appropriately,[5] whereas the fluorine A5Z set was completely decontracted.

Basis set superposition errors (BSSE) with respect to the energy are rather small. For instance, the $X^6\Delta$ state of FeF is about 0.6 and 0.3 kcal/mol, as calculated by the counterpoise method,[12] at all levels of correlated theories using the 4Z and 5Z (or C5Z) basis sets, respectively. Finally, size nonextensivity errors concerning the CI calculations were mitigated by applying the supermolecule approach (interatomic distances of ∼50 bohr) in calculating binding energies along with the Davidson (+Q) correction for unlinked clusters.[13]

In the present work, we have examined the electronic structure of a total of 35 low-lying states of FeF (6), CoF (11), NiF (11), and CuF (7). Complete potential energy curves (PEC) have been constructed for 29 states at the MRCI/4Z level; we present dissociation energies, common spectroscopic parameters (r_e, ω_e, $\omega_e x_e$, α_e), and dipole moments calculated as expectation values ($\langle\mu\rangle$) and through the finite field approach (μ_{FF}).

Almost all of our calculations have been performed by the MOLPRO 2006.1 code;[8] the ACESII program was also used for certain states.[14]

3. The Atoms

Table 1 collects the ionization energies (IE) of Fe, Co, Ni, and Cu, whereas Table 2 lists energy separations of the three lowest states of the corresponding cations at the MRCI and CC methods, using the ANO[4] and the Balabanov−Peterson[5] quintuple-ζ basis sets; the three lowest M^+ states are involved in the molecular MF calculations. At the highest-level C-MRCI+DKH2+Q (C-RCCSD(T)+DKH2)/CBP, the agreement with experimental IEs is quite good, the largest discrepancy being that of Cu, +0.29 (−0.041) eV. We observe that as we increase the level of calculation, IEs converge monotonically to the experimental values. For a systematic and high-level study of the IEs of the series Sc−Zn, we refer to the recent work of Balabanov and Peterson.[5b] Unfortunately, we cannot say the same for the first two energy separations of M^+, where the agreement with experiment cannot be considered as good, even at the highest level of calculation, be it MRCI or CC, Table 2. It is interesting that in Co^+, the ground state is predicted to be $^5F(4s^13d^7)$ instead of $^3F(3d^8)$ at the C-MRCI+DKH2/CBP level. A large discrepancy is also calculated at the same level in the $^4F(4s^13d^8) \leftarrow {}^2D(3d^9)$ difference of Ni^+, but the situation is mitigated significantly for both Co^+ and Ni^+ by including the Davidson correction. Overall, we can say that the results at the CC level are better as contrasted to the MRCI ones.

Finally, the CISD+Q (RCCSD(T))/A5Z electron affinity (EA) of fluorine is calculated to be 3.26 (3.404) eV, the experimental value being 3.401190 eV.[15a]

4. Results and Discussion

A. FeF. As early as 30 years ago, Pouilly et al. established the ground-state symmetry of FeF, $^6\Delta_{i,9/2}$, through rotational spectroscopy.[16a] Limited ab initio CISD calculations by the same authors confirmed the assignment of the X state.[16b] In 1996, Ram et al. by Fourier transform spectroscopy observed two excited quartets $a^4\Delta$ and $g^4\Delta$.[17] Allen and Ziurys confirmed the ground state of FeF as $^6\Delta_i$ by pure rotational spectroscopy[18] and obtained, among other parameters, an accurate bond distance $r_e = 1.7803$ Å.[18b] Two more experimental works appeared more recently, where via fluorescence spectroscopy, Kermode and Brown probed the $X^6\Delta$ and a limited number of excited states.[19] Finally, the binding energy of FeF has been estimated to be $D_e = 107 \pm 5$ kcal/mol through high-temperature mass spectroscopy.[20] Relative experimental results from refs 16−20 will be contrasted with our own later on.

On the theoretical side, besides the work of Pouilly et al.,[16b] the only relatively recent ab initio study on FeF is by Bauschlicher, who examined the $^6\Delta$, $^4\Delta$, $^4\Phi$, and $^4\Sigma^-$ states of FeF by CCSD(T) and MCPF (modified coupled pair functional)/[8s7p4d3f2g/$_{Fe}$AQZ/$_F$] methods.[21]

Table 3 collects our numerical results, whereas MRCI/4Z PECs of six low-lying states, $X^6\Delta$, $A^6\Pi$, $a^4\Delta$, $B^6\Sigma^+$, $b^4\Pi$, and

TABLE 2: Energy Separations (eV) of the Three Lowest States of the Fe^+, Co^+, Ni^+, and Cu^+ Cations by Different Methods and Basis Sets

	Fe^+		Co^+		Ni^+		Cu^+	
method/basis set[a]	$^4F \leftarrow {}^6D$	$^4D \leftarrow {}^6D$	$^5F \leftarrow {}^3F$	$^3F \leftarrow {}^3F$	$^4F \leftarrow {}^2D$	$^2F \leftarrow {}^2D$	$^3D \leftarrow {}^1S$	$^1D \leftarrow {}^1S$
MRCI/ANO	0.413	1.146	0.248	1.210	0.867	1.610	2.412	2.840
MRCI+Q	0.195	1.031	0.563	1.438	1.284	1.973	3.156	3.575
RCCSD(T)/ANO	0.200		0.567		1.297		3.164	
MRCI/BP	0.356	1.139	0.290	1.236	0.894	1.634	2.431	2.858
MRCI+Q	0.141	1.020	0.596	1.454	1.313	1.993	3.158	3.574
RCCSD(T)/BP	0.137		0.608		1.342		3.195	
C-MRCI+DKH2/CBP	0.770	1.348	−0.215	0.881	0.273	1.103	1.647	2.117
C-MRCI+DKH2+Q	0.447	1.132	0.206	1.153	0.813	1.554	2.506	2.960
C-RCCSD(T)+DKH2/CBP	0.326		0.366		1.041		2.783	
expt.[b]	0.248	0.980	0.429	1.212	1.085	1.682	2.808	3.256

[a] ANO = [7s6p4d3f2g], BP = [9s8p6d4f3g2h1i], CBP = [11s10p8d5f4g3h2i]; +Q refers to the Davidson correction and DKH2 to second-order Douglas−Kroll−Hess scalar relativistic corrections. [b] Ref 15b.

TABLE 3: Total Energies E (E_h), Equilibrium Bond Distances r_e (Å), Dissociation Energies with Respect to the Ground-State Atoms D_e (kcal/mol), Harmonic and Anharmonic Frequencies ω_e, $\omega_e x_e$ (cm^{-1}), Rotational−Vibration Constants α_e (cm^{-1}), Zero Point Energies ZPE (cm^{-1}), Dipole Moments μ_e (D), Mulliken Charges Q_{Fe}, and Energy Separations T_e (cm^{-1}) of FeF

method/basis set[a]	$-E$	r_e	D_e	ω_e	$\omega_e x_e$	α_e	ZPE	$\langle\mu\rangle$ (μ_{FF})[b]	Q_{Fe}	T_e
				$X^6\Delta$						
MRCI/4Z	1362.44501	1.8011	109.3	649.5	3.2	0.0027	324.1	2.56 (2.61)	0.73	0.0
MRCI+Q	1362.4791	1.796	110.6	652.0	3.2	0.0028	325.4			0.0
MRCI/5Z	1362.46122	1.7990	109.7	651.9	3.2	0.0026	325.2	2.50 (2.54)	0.73	0.0
MRCI+Q	1362.4960	1.794	111.2	654.1	3.2	0.0027	326.3			0.0
MRCI+DKH2/5Z	1371.43098	1.7957	107.5	647.9	2.0	0.0029	324.1	2.52 (2.59)	0.73	0.0
MRCI+DKH2+Q	1371.4662	1.791	108.9	654.8	3.3	0.0027	326.7			0.0
C-MRCI/C5Z	1362.86235	1.7966	108.5	654.8	3.3	0.0028	326.7	2.56 (2.62)	0.81	0.0
C-MRCI+Q	1362.9415	1.791	111.3	660.1	4.2	0.0030	329.0			0.0
C-MRCI+DKH2/C5Z	1371.83264	1.7928	106.3	656.8	3.3	0.0025	327.5	2.57 (2.64)	0.80	0.0
C-MRCI+DKH2+Q	1371.9122	1.787	108.9	656.0	2.3	0.0028	327.9			0.0
RCCSD(T)/4Z	1362.49216	1.7932	111.0	653.7	3.3	0.0027	326.1	(2.41)		0.0
RCCSD(T)/5Z	1362.50986	1.7908	111.6	655.3	3.1	0.0027	327.0	(2.37)		0.0
RCCSD(T)+DKH2/5Z	1371.48019	1.7876	109.3	653.9	2.6	0.0028	326.7	(2.36)		0.0
C-RCCSD(T)/C5Z	1362.97248	1.7859	111.0	660.0	3.1	0.0028	329.4	(2.41)		0.0
C-RCCSD(T)+DKH2/C5Z	1371.943509	1.7833	108.7	660.0	2.6	0.0026	329.3	(2.48)		0.0
CCSD(T)/4Z[c]		1.794	110.1	651						
expt.			107 ± 5[d]							
		1.78063[e]		663.2[e]	3.38[e]					
				$A^6\Pi$						
MRCI/4Z	1362.42612	1.8421	97.6	616.5	3.1	0.0027	307.6	3.00 (3.11)	0.74	4146
MRCI+Q	1362.4597	1.839	98.4	617.4	3.1	0.0027	308.0			4249
C-MRCI+DKH2/C5Z	1371.81321	1.8349	94.5	623.2	3.1	0.0024	310.8	3.02 (3.14)	0.81	4264
C-MRCI+DKH2+Q	1371.8922	1.831	96.6				310.2			4402
RCCSD(T)/4Z	1362.47250	1.8360	98.7	617.3	2.9	0.0026	308.1	(2.86)		4316
C-RCCSD(T)+DKH2/C5Z	1371.92324	1.8281	95.9	623.9	4.0	0.0031	311.0	(3.00)		4449
expt.[f]										~4660
				$a^4\Delta$						
MRCI/4Z	1362.42073	1.7755	94.0	662.7	3.3	0.0027	330.6	2.55 (3.18)	0.67	5327
MRCI+Q	1362.4571	1.767	96.8	666.5	3.3	0.0027				4833
C-MRCI+DKH2/C5Z	1371.80563	1.7677	89.3	669.5	3.3	0.0023	333.7	2.46 (3.14)	0.78	5928
C-MRCI+DKH2+Q	1371.8875	1.758	93.4	671.6	3.0	0.0029	335.4			5424
CCSD(T)4Z[c]		1.753	96.5	680						
expt.[g]		1.7392		684.2 ($\Delta G_{1/2}$)		0.0028				
				$B^6\Sigma^+$						
MRCI/4Z	1362.41735	1.8425	92.6	592.8	2.8	0.0027	296.0	2.92 (3.10)	0.75	6069
MRCI+Q	1362.4533	1.831	94.5	598.5	3.0	0.0027	298.6			5667
C-MRCI+DKH2/C5Z	1371.80460	1.8334	88.7	599.6	2.8	0.0024	299.1	2.91 (3.13)	0.81	6153
C-MRCI+DKH2+Q	1371.8859	1.822	92.4	608.0	4.5	0.0027	303.0			5784
RCCSD(T)/4Z	1362.46902	1.8157	96.5	597.9				(2.73)		5078
C-RCCSD(T)+DKH2/C5Z	1371.92186	1.7981	95.1	622.3	4.2	0.0027	309.5	(2.67)		4752
expt.[f]		1.7829 (r_0)		595 ($\Delta G_{1/2}$)						4828.6 (T_0)
				$b^4\Pi$						
MRCI/4Z	1362.40524	1.8052	84.5	633.2	3.2	0.0027	316.0	3.00 (3.45)	0.69	8727
MRCI+Q	1362. 4415	1.797	86.9	635.9	3.3	0.0027	317.2			8248
C-MRCI+DKH2/C5Z	1371.79000	1.7936	79.9	638.2	2.7	0.0025	318.6	2.95 (3.43)	0.80	9357
C-MRCI+DKH2+Q	1371.8718	1.785	83.7	644.6	4.2	0.0031	321.2			8880
				$c^4\Sigma^+$						
MRCI/4Z	1362.38743	1.8514	73.8	596.4	2.9	0.0026	297.7	2.62 (2.67)	0.70	12637
MRCI+Q	1362.4243	1.843	76.3	600.0	3.0	0.0027	299.4			12024
C-MRCI+DKH2/C5Z	1371.77172	1.8396	68.9	604.3	3.3	0.0025	301.3	2.57 (2.58)	0.80	13370
C-MRCI+DKH2+Q	1371.8538	1.832	72.6	602.4	2.3	0.0028	301.0			12829

[a] +Q and DKH2 refer to the Davidson correction and to second-order Douglas−Kroll−Hess scalar relativistic corrections. C- means that the metal semicore $3s^23p^6$ e^- have been correlated. [b] $\langle\mu\rangle$ was calculated as an expectation value and μ_{FF} via the finite field approach. The field strength was 2×10^{-5} au. [c] Ref 21. [d] Ref 20. [e] Ref 19a. [f] Ref 19b. [g] Ref 17.

$c^4\Sigma^+$ spanning an energy range of 1.6 eV, are displayed in Figure 1 along with an inset displaying relative energies.

$X^6\Delta$. Our calculations confirm beyond any doubt that the ground state of FeF is of $^6\Delta$ symmetry, with the first excited state $A^6\Pi$ considerably higher. As the quality of the calculations improves from MRCI/4Z to C-MRCI+DKH2+Q/C5Z and correspondingly from RCCSD(T)/4Z to C-RCCSD(T)+DKH2/C5Z, the bond distance converges to the experimental value, r_e = 1.78063 Å.[19a] In particular, at the highest MRCI (CC) level, we obtain r_e = 1.787 (1.7833) Å, in very good agreement with experiment. The adiabatic dissociation energy D_e with respect to Fe(^{5}D) + F(^{2}P) is practically insensitive to the level of calculation. We observe that upon including relativistic effects in both MRCI or CC, with or without the "core" (~$3s^23p^6$) Fe electrons, D_e decreases by 2.3 kcal/mol with a minor effect due to the core electrons alone. Our best MRCI (CC) value is 108.9

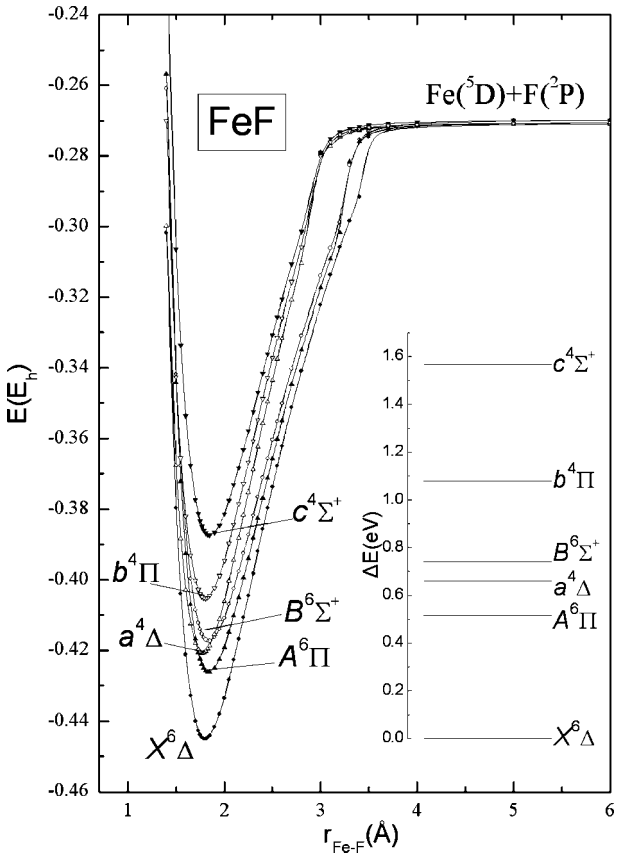

Figure 1. MRCI/4Z potential energy curves of the FeF molecule and relative energy level diagram inset. All energies are shifted by +1362.0 E_h.

(108.7) kcal/mol; including the ZPE and BSSE (0.3 kcal/mol in both MRCI or CC), $D_0 = 107.7$ (107.5) kcal/mol. We suggest, as our best "estimate", that $D_0 = 108$ kcal/mol, certainly better focused than the experimental value of 107 ± 5 kcal/mol.[20] Diabatically, $D_e^d = D_e$ + IE(Fe→Fe$^+$) + EA(F$^-$←F) = 109 kcal/mol + 7.865 eV − 3.38 eV = 212 kcal/mol, where IE and EA are the ionization energy and the electron affinity of Fe and F, respectively, at the highest CC level. The D_e^d value should be contrasted to 187 kcal/mol, assuming a purely Coulombic interaction at $r_e = 1.78$ Å. Observe also that the PECs of all states (Figure 1) suffer an avoided crossing in the narrow range of 3.0−3.5 Å resulting from the interaction with the ionic states Fe$^+$F$^-$, its accurate position depending on the Fe$^+$ term. The position of the avoided crossing (r_{ac}) is practically dictated from the IE − EA difference, that is, $r_{ac} = (\text{IE} - \text{EA})^{-1} = 6.7$ au = 3.20 Å for the X$^6\Delta$ state, the calculated MRCI/4Z value being close to 3.4 Å.

The CASSCF/4Z equilibrium configuration function (CF) and atomic Mulliken populations of the X$^6\Delta$ state are (Fe/F)

$$|X^6\Delta\rangle_{A_2} = 0.997|(\text{core})^{20}1\sigma^2 2\sigma^2 1\pi_x^2 1\pi_y^2 3\sigma^1 4\sigma^1 2\pi_x^1 2\pi_y^1 1\delta_+^1 1\delta_-^2\rangle$$

$$4s^{0.94}4p_z^{0.22}3d_{z^2}^{1.02}3d_{xz}^{1.02}3d_{yz}^{1.01}3d_{x^2-y^2}^{1.00}3d_{xy}^{2.00}/2s^{1.97}2p_z^{1.84}2p_z^{1.96}2p_y^{1.96}$$

where (core)^{20} refers to the 20 inner e$^-$ of Fe(∼1s^{2}2s^{2}2p^{6}3s^{2}3p^6) + F(∼1s^2). Overall, 0.7−0.8 e$^-$ are transferred from Fe to F. The orbitals $1\sigma^2$, $2\sigma^2$, $1\pi_x^2$, and $1\pi_y^2$ describe the eight "valence" electrons of F$^-$. Hence, for the MF states presently studied, we can approximately write, albeit in a very good approximation, $|MF\rangle \approx \hat{A}|M^+\rangle \times |F^-\rangle$, suppressing the common factor (core)$^{20}1\sigma^2 2\sigma^2 1\pi_x^2 1\pi_y^2$. The remaining electrons determine the $|M^+\rangle$ state, which, in turn, defines the symmetry of the MF states (see also ref 1). Following this convention, we can write for the X state of FeF

$$|X^6\Delta\rangle_{A_2} = 0.997|3\sigma^1 4\sigma^1 2\pi_x^1 2\pi_y^1 1\delta_+^1 1\delta_-^2\rangle$$

According to the above, the bonding can be described by the following valence-bond-Lewis (vbL) scheme.

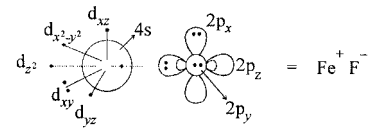

(1)

$Fe^+(^6D; M_L=\pm2)$ $F^-(^1S)$ $X^6\Delta$

Due to the highly ionic character of the MF species, dipole moments are almost invariant to the method of calculation (see also ref 1). In the case of the X$^6\Delta$ of FeF, we can claim that the value of the dipole moment is $\mu = 2.55 \pm 0.05$ D (Tabe 3). It should also be said that in all MF species and states (M = Sc−Cu), μ values are very high at the inflection points due to the avoided crossings with the M$^+$F$^-$ states, ranging from 19 (TiF; X$^4\Phi$)[1] to 9 D (CuF; X$^1\Sigma^+$), and then diminish linearly as we approach the equilibrium distance.

As was already mentioned, the $^{2S+1}|\Lambda|$ MF states expected are determined from the M$^+$ terms in the field of the F$^-$ anion. The ground state of Fe$^+$ (^{6}D) gives rise to $^6\Sigma^+$, $^6\Pi$, and $^6\Delta$ states, the last one being the ground state of FeF. The next state of Fe$^+$, ^{4}F, is located 0.248 eV (M_j averaged) higher[15b] giving rise to $^{2S+1}|\Lambda|$ states of $^4\Sigma^-$, $^4\Pi$, $^4\Delta$, and $^4\Phi$ symmetries. At 0.980 eV, the ^{4}D term of Fe$^+$ is related to the $^4\Sigma^+$, $^4\Pi$, and $^4\Delta$ molecular states. It is expected that the two sextets, $^6\Sigma^+$, and $^6\Pi$, are the first two lowest states followed by the quartets. Presently, we have calculated the $^6\Sigma^+$and $^6\Pi$, in addition to X$^6\Delta$, and the three quartets correlating to the ^{4}D term of Fe$^+$. The four quartets, $^4\Sigma^-$, $^4\Pi$, $^4\Delta$, and $^4\Phi$ emanating from the ^{4}F term of Fe$^+$, are located higher and have not been examined. The ordering of the calculated states is X$^6\Delta$, A$^6\Pi$, a$^4\Delta$, B$^6\Sigma^+$, b$^4\Pi$, c$^4\Sigma^+$ (see Figure 1); however, as the level of the calculation improves, the a$^4\Delta$ and B$^6\Sigma^+$ tend to become degenerate (see below). We discuss now the $^6\Sigma^+$ and $^6\Pi$ followed by the three quartets.

***B*$^6\Sigma^+$, *A*$^6\Pi$.** Both states were observed for the first time in 2002 by fluorescence spectroscopy.[19b] The energy distance T(A$^6\Pi$←X$^6\Delta$) is the only experimental datum for the A$^6\Pi$ state, where, for the B$^6\Sigma^+$, the values of r_0, $\Delta G_{1/2}$ and T_0 have been also determined.[19b] Following the previous convention, the CASSCF CFs are $|A^6\Pi\rangle_{B_1} = 0.997|3\sigma^1 4\sigma^1 2\pi_x^2 2\pi_y^1 1\delta_+^1 1\delta_-^1\rangle$ and $|B^6\Sigma^+\rangle_{A_1} = 0.997|3\sigma^2 4\sigma^1 2\pi_x^1 2\pi_y^1 1\delta_+^1 1\delta_-^1\rangle$, impressively of single reference character and similar to the X$^6\Delta$ state, with the in situ metal atom as Fe$^+$(^{6}D; $M_L = \pm1$) and Fe$^+$(^{6}D; $M_L = 0$). The bonding, clearly "Coulombic" as in the X state, is represented graphically by the scheme (1) but with the $3d_{xy}(\delta_-)$ electron pair moved to the $3d_{z^2}(3\sigma)$ orbital (B$^6\Sigma^+$) or to the $3d_{xz}(2\pi_x)$ orbital (A$^6\Pi$).

The C-MRCI+DKH2+Q [C-RCCSD(T)+DKH2]/C5Z T_e of the A$^6\Pi$ state is in harmony with the experimental value; the same can be said, at least, at the C-RCCSD(T)+DKH2/C5Z level for the B$^6\Sigma^+$ state (Table 3). In the latter, the bond distance decreases monotonically as we move from the MRCI/4Z to the highest CC level, the final r_e value differing from the experimental one by 0.015 Å.[19b] However, according to the authors of ref 19b, the bond distance of the B$^6\Sigma^+$ state, "cannot be regarded as definitive". As to the dipole moments, the $\langle\mu\rangle$ and

μ_{FF} MRCI values are the same, 3.0 and 3.1 D for both states; considering the CC results as more reliable, however, our recommended μ values are 3.0 ($A^6\Pi$) and 2.7 D ($B^6\Sigma^+$).

***c*$^4\Sigma^+$, *b*$^4\Pi$, *a*$^4\Delta$.** The quartets correlate diabatically to the second excited state of Fe^+ (^4D; $M_L = 0, \pm1, \pm2$) + $F^-(^1S)$ but adiabatically to the ground-state atoms due to the avoided crossing at 3.2 Å with the ionic $Fe^+(^4D)F^-(^1S)$ state (vide supra). The CASSCF equilibrium wave functions are indicative of their intense multireference character; thus, CC calculations have not been tried. The leading equilibrium CASSCF configurations are

$$|a^4\Delta\rangle_{A_1} = |[0.53(3\sigma^1 4\bar{\sigma}^1 1\delta_+^2) - 0.51(3\sigma^2 1\delta_+^2) + 0.32(4\sigma^2 1\delta_+^2)](2\pi_x^1 2\pi_y^1 1\delta_-^1) - (3\sigma^1 4\sigma^1 1\delta_+^2)[0.44(2\bar{\pi}_x^1 2\pi_y^1 1\delta_-^1) + 0.31(2\pi_x^1 2\bar{\pi}_y^1 1\delta_-^1) + 0.25(2\pi_x^1 2\pi_y^1 1\bar{\delta}_-^1)]\rangle$$

$$|b^4\Pi\rangle_{B_1} = |[0.68(3\sigma^2 1\delta_+^1) - 0.46(4\sigma^2 1\delta_+^1) + 0.37(3\sigma^1 4\sigma^1 1\bar{\delta}_+^1) - 0.21(3\sigma^1 4\bar{\sigma}^1 1\delta_+^1)](2\pi_x^2 2\pi_y^1 1\delta_-^1) + (3\sigma^1 4\sigma^1 2\pi_x^2 1\delta_+^1)[0.29(2\bar{\pi}_y^1 1\delta_-^1) + 0.24(2\pi_y^1 1\bar{\delta}_-^1)]\rangle$$

$$|c^4\Sigma^+\rangle_{A_1} = |[0.76(3\sigma^2 4\bar{\sigma}^1 1\delta_+^1) - 0.22(3\sigma^1 4\sigma^2 1\bar{\delta}_+^1)](2\pi_x^1 2\pi_y^1 1\delta_-^1) - (3\sigma^2 4\sigma^1 1\delta_+^1)[0.43(2\bar{\pi}_x^1 2\pi_y^1 1\delta_-^1) + 0.31(2\pi_x^1 2\bar{\pi}_y^1 1\delta_-^1) + 0.24(2\pi_x^1 2\pi_y^1 1\bar{\delta}_-^1)]\rangle$$

The ordering of the states is $a^4\Delta$, $b^4\Pi$, and $c^4\Sigma^+$ with C-MRCI+DKH2+Q/C5Z T_e values of 5424, 8880, and 12829 cm^{-1}, respectively, and the $B^6\Sigma^+$ state in between the $a^4\Delta$ and $b^4\Pi$. Notice that as the level of calculation improves, the $a^4\Delta - B^6\Sigma^+$ energy interval diminishes, the final value being 360 cm^{-1}.

An interesting variation is observed in the $\langle\mu\rangle$ and μ_{FF} dipole moments of the $a^4\Delta$ and $b^4\Pi$ states: the μ_{FF} values are about 0.7 and 0.5 D larger than the corresponding $\langle\mu\rangle$ values; as it has been discussed before, we tend to trust more the finite field rather than the expectation values.[22]

B. CoF. To the best of our knowledge, no theoretical results exist on CoF; on the other hand, the experimental pedigree on the ground state of the molecule is intriguing. The first experimental work on CoF appeared 30 years ago by DeVore et al., claiming that its ground state is of $^3\Pi$ symmetry.[23] After a paucity of 16 years, a series of six papers has been published, all suggesting that the ground state is of $^3\Phi$ symmetry.[24−28] Notwithstanding the agreement among the different groups on the ground-state symmetry of CoF, conceptual differences have been also expressed on the origin of the $^3\Phi$ state. It is interesting to examine at this point some of the details of this disagreement. CoF is, with no doubt, an ionic system, similar to all MF (M = Sc−Cu) molecules; hence, the molecular states produced are dictated by the M^+ terms. The ground state of Co^+ is $^3F(d^8)$, with a $^5F(4s^13d^7)$ and a $^3F(4s^13d^7)$ state of 0.429 and 1.212 eV higher, respectively.[15b] In the field of the $F^-(^1S)$ anion, these Co^+ states give rise to a series of $^{2S+1}|\Lambda|$ molecular states, all of the same spatial symmetries, triplets and quintets: $Co^+(^3F; 3d^8) + F^-(^1S) \rightarrow {}^3\Sigma^-, {}^3\Pi, {}^3\Delta, {}^3\Phi$; $Co^+(^5F; 3d^74s^1) + F^-(^1S) \rightarrow {}^5\Sigma^-, {}^5\Pi, {}^5\Delta, {}^5\Phi$; $Co^+(^3F; 3d^74s^1) + F^-(^1S) \rightarrow {}^3\Sigma^-, {}^3\Pi, {}^3\Delta, {}^3\Phi$. In refs 25 and 26, it is suggested that the $X^3\Phi$ state of CoF traces its diabatic origin to the ground state of $Co^+(^3F; 3d^8)$, that is, the in situ symmetry of Co^+. The argument is based on the "analogy" between CoF and CoH ($X^3\Phi$). On the contrary, Steimle et al.,[28] using laser-induced fluorescence spectroscopy, express their confidence that the in situ Co^+ in $X^3\Phi$ is in the $Co^+(^3F; 3d^74s^1)$ state. As a matter of fact, in ref 28, it is stated that, "...the analogy between CoF and CoH should definitely be reconsidered".

The $M_L = 0, \pm1, \pm2$, and ±3 components of the ground and the first excited states of Co^+, $^3F(d^8)$ and $^5F(s^1d^7)$, are (in an obvious notation)

$$|^3F;0\rangle = \sqrt{4/5}|d_{xz}^1 d_{yz}^1\rangle - \sqrt{1/5}|d_{x^2-y^2}^1 d_{xy}^1\rangle$$

$$|^3F;\pm1\rangle_{B1} = \sqrt{2/5}|d_{z^2}^1 d_{xz}^1\rangle - \sqrt{3/10}|d_{xz}^1 d_{x^2-y^2}^1\rangle + \sqrt{3/10}|d_{yz}^1 d_{xy}^1\rangle$$

$$|^3F;\pm2\rangle_{A_1} = |d_{z^2}^1 d_{x^2-y^2}^1\rangle$$

$$|^3F;\pm3\rangle_{B_1} = \sqrt{1/2}(|d_{xz}^1 d_{x^2-y^2}^1\rangle + |d_{yz}^1 d_{xy}^1\rangle)$$

$$|^5F;0\rangle = (\sqrt{4/5}|d_{z^2}^1 d_{x^2-y^2}^1 d_{xy}^1\rangle - \sqrt{1/5}|d_{z^2}^1 d_{xz}^1 d_{yz}^1\rangle)|s^1\rangle$$

$$|^5F;\pm1\rangle_{B_1} = (\sqrt{2/5}|d_{yz}^1 d_{x^2-y^2}^1 d_{xy}^1\rangle + \sqrt{3/10}|d_{z^2}^1 d_{xz}^1 d_{x^2-y^2}^1\rangle + \sqrt{3/10}|d_{z^2}^1 d_{yz}^1 d_{xy}^1\rangle)|s^1\rangle$$

$$|^5F;\pm2\rangle_{A_1} = |d_{xz}^1 d_{yz}^1 d_{xy}^1\rangle|s^1\rangle$$

$$|^5F;\pm3\rangle_{B_1} = \sqrt{1/2}(|d_{z^2}^1 d_{xz}^1 d_{x^2-y^2}^1\rangle - |d_{z^2}^1 d_{yz}^1 d_{xy}^1\rangle)|s^1\rangle$$

The $^3\Sigma^-$, $^3\Delta$, and $^3\Phi$ states correlating diabatically to $Co^+(^3F;d^8)$ have been examined at the CC level but not the $^3\Pi$ ($M_L = \pm1$) due to its multireference character. At the MRCI level, these states appear relatively high in energy; as a result, their calculation was practically forbidden. The quintets $^5\Sigma^-$, $^5\Pi$, $^5\Delta$, and $^5\Phi$ correlating to $Co^+(^5F;s^1d^7)$ have been examined at both the MRCI and CC levels, with the exception of the $^5\Pi$ ($M_L = \pm1$) state, which is not tractable at CC.

Finally, states related to the $Co^+(s^1d^7)$ located 1.212 eV higher,[15b] that is, $^3\Sigma^-$, $^3\Pi$, $^3\Delta$, and $^3\Phi$, have been tackled at the MRCI level because of their extreme multireference description, as is obvious from the M_L components of the low-spin (triplet) configuration of Co^+ (^3F; s^1d^7).

According to the discussion above, we have examined a total of 11 states but not all of them in an equal basis; this, of course, this makes comparison among the states difficult and problematic. Table 4 collects all numerical results, and Figure 2 displays PECs of eight states at the MRCI/4Z level of theory. The level diagram depicted in Figure 3 indicates clearly the difficulties faced with the CoF system.

According to the C-MRCI+DKH2+Q/C5Z results, which do not differ significantly from the corresponding MRCI/4Z (see Table 4 and Figures 2 and 3), the ground state is of $^5\Phi(s^1d^7)$ symmetry with the first excited state, $^5\Sigma^-(s^1d^7)$, located 1477 cm^{-1} (=4.22 kcal/mol) higher, followed by two quintets, $^5\Pi(s^1d^7)$ and $^5\Delta(s^1d^7)$, at $T_e = 2054$ and 2241 cm^{-1}, respectively. The next state of $^3\Phi(s^1d^7)$ symmetry with $T_e = 3138$ cm^{-1} is, according to the experimental results of Steimle et al.,[28] the ground state of CoF. Our MRCI results hardly suggest the $^3\Phi(s^1d^7)$ as the lowest state (but see below). Experimentally, we do know that $\Delta E_0(^3\Delta - ^3\Phi) = 4005.02$ cm^{-1}, but their origin (s^1d^7 or d^8) is unclear.[25b] At the MRCI/4Z (C-MRCI+DKH2+Q/C5Z) level $\Delta E_0(^3\Delta - ^3\Phi) = 4378$ (4559) cm^{-1}, in fairly good agreement with the experiment, indicating that we are in the s^1d^7 manifold. Experimental bond distances (r_e) are 1.7349[25b] or 1.73810[26] Å for the $^3\Phi$ state, and $r_0 = 1.78487$ Å for the

TABLE 4: Total Energies E (E_h), Equilibrium Bond Distances r_e (Å), Dissociation Energies with Respect to the Ground-State Atoms D_e (kcal/mol), Harmonic and Anharmonic Frequencies ω_e, $\omega_e x_e$ (cm^{-1}), Rotational−Vibration Constants α_e(cm^{-1}), Zero Point Energies ZPE(cm^{-1}), Dipole Moments μ_e (D), Mulliken Charges Q_{Co}, and Energy Separations T_e (cm^{-1}) of CoF

method/basis set[a]	$-E$	r_e	D_e	ω_e	$\omega_e x_e$	α_e	ZPE	$\langle\mu\rangle$ (μ_{FF})[b]	Q_{Co}	T_e
MRCI Results										
				$^5\Phi(s^1d^7)$						
MRCI/4Z	1481.45477	1.7935	99.1	647.9	3.2	0.0027	323.1	2.75 (2.86)	0.69	0.0
MRCI+Q	1481.4939	1.790	100.4	647.5	2.8	0.0028	323.7			0.0
MRCI/5Z	1481.47525	1.7915	99.5	651.9	5.4	0.0030	324.1	2.69 (2.80)	0.74	0.0
MRCI+Q	1481.5154	1.788	100.9	651.5	3.5	0.0027	324.8			0.0
MRCI+DKH2/5Z	1492.00326	1.7882	96.8	649.2	3.0	0.0027	324.1	2.71 (2.86)	0.74	0.0
MRCI+DKH2+Q	1492.0439	1.785	98.1	650.1	2.5	0.0027	324.8			0.0
C-MRCI/C5Z	1481.88633	1.7905	98.2	652.9	3.6	0.0027	325.5	2.74 (2.85)	0.81	0.0
C-MRCI+Q	1481.9708	1.786	100.8	655.8	4.0	0.0027	326.7			0.0
C-MRCI+DKH2/C5Z	1492.41505	1.7872	95.5	652.7	3.3	0.0027	325.6	2.76 (2.86)	0.80	0.0
C-MRCI-DKH2+Q	1492.5001	1.783	97.9	654.8	3.4	0.0026	326.6			0.0
				$^5\Sigma^-(s^1d^7)$						
MRCI/4Z	1481.44658	1.7969	95.0	628.8	3.0	0.0026	313.8	2.77 (2.92)	0.69	1798
MRCI+Q	1481.4862	1.791	96.2	628.1	2.9	0.0026	313.5			1697
C-MRCI+DKH2/C5Z	1492.40757	1.7909	91.5					2.76	0.80	1642
C-MRCI-DKH2+Q	1492.4934	1.784	93.9							1477
				$^5\Pi(s^1d^7)$						
MRCI/4Z	1481.44486	1.8078	93.3	629.2	3.1	0.0027	314.0	2.88 (2.98)	0.69	2175
MRCI+Q	1481.4845	1.803	94.6	630.6	3.2	0.0027	315.3			2081
C-MRCI+DKH2/C5Z	1492.40524	1.8012	89.7					2.88	0.81	2152
C-MRCI-DKH2+Q	1492.4908	1.796	92.2							2054
				$^5\Delta(s^1d^7)$						
MRCI/4Z	1481.44354	1.8109	91.6	616.6	3.0	0.0027	307.8	2.84 (2.92)	0.69	2464
MRCI+Q	1481.4838	1.803	93.6	620.1	3.1	0.0027	309.7			2238
C-MRCI+DKH2/C5Z	1492.40386	1.8017	88.2					2.83	0.80	2455
C-MRCI-DKH2+Q	1492.4899	1.793	91.2							2241
				$^3\Phi(s^1d^7)$[c]						
MRCI/4Z	1481.43995	1.7559	89.8	665.3	3.1	0.0028	332.1	2.94 (3.68)	0.65	3254
MRCI+Q	1481.4820	1.747	92.9	668.6	3.5	0.0031	334.0			2620
C-MRCI+DKH2/C5Z	1492.39788	1.7485	84.7	670.1	3.3	0.0027	334.3	2.88	0.79	3767
C-MRCI-DKH2+Q	1492.4858	1.738	88.9	674.5	3.3	0.0027	336.4			3138
expt.		**1.7349[d]/1.7381[e]**		677.59[d]						
				$^3\Sigma^-(s^1d^7)$						
MRCI/4Z	1481.42933	1.7703	84.2	644.2	2.9	0.0027	321.7	2.72 (3.43)	0.64	5583
MRCI+Q	1481.4719	1.760	87.2	648.3	4.0	0.0028	323.2			4831
C-MRCI+DKH2/C5Z	1492.38788	1.7632	79.1	651.9	4.0	0.0028	324.9	2.63	0.78	5963
C-MRCI-DKH2+Q	1492.4766	1.753	83.3	651.0	3.1	0.0030	324.9			5155
				$^3\Pi(s^1d^7)$						
MRCI/4Z	1481.42798	1.7756	82.7	638.6	3.1	0.0027	318.9	2.94 (3.50)	0.66	5880
MRCI+Q	1481.4703	1.766	85.7	641.9	3.2	0.0028	320.2			5195
C-MRCI+DKH2/C5Z	1492.38602	1.7682						2.90 (3.40)		6371
C-MRCI-DKH2+Q	1492.4742	1.757								5684
				$^3\Delta(s^1d^7)$[c]						
MRCI/4Z	1481.42000	1.8134	76.9	619.9	3.0	0.0027	309.4	2.59 (2.67)	0.66	7632
MRCI+Q	1481.4611	1.807	79.4	623.1	3.6	0.0027	310.6			7208
C-MRCI+DKH2/C5Z	1492.37815	1.8033	72.0	625.9	3.3	0.0027	312.1	2.54	0.79	8100
C-MRCI-DKH2+Q	1492.4651	1.797		628.7	3.6	0.0028	313.4			7697
expt.[d]		1.78487								
RCCSD(T) Results										
				$^3\Phi(d^8)$						
RCCSD(T)/4Z	1481.50305	1.7524	95.9	655.0	3.9	0.0030	326.6			0.0
RCCSD(T)/5Z	1481.52621	1.7506	96.8							0.0
C-RCCSD(T)+DKH2/C5Z	1492.52782	1.7358	92.3	669.1	3.9	0.0032	333.7	(4.61)		0.0
				$^5\Delta(s^1d^7)$						
RCCSD(T)/4Z	1481.50099	1.7948	94.6	623.1	3.6	0.0028	310.6	(2.85)		452
C-RCCSD(T)+DKH2/C5Z	1492.52771	1.7815	92.3	628.5	2.6	0.0028	313.9			24
				$^5\Phi(s^1d^7)$						
RCCSD(T)/4Z	1481.50310	1.7871	96.0	649.9	3.4	0.0026	324.1	(2.61)		−11
RCCSD(T)/5Z	1481.52550	1.7848	96.4	650.1	2.9	0.0028	324.6	(2.55)		156
RCCSD(T)+DKH2/5Z	1492.05431	1.7815	93.6	648.7	2.5	0.0031	324.2	(2.5)		
C-RCCSD(T)/C5Z	1481.99768	1.7813	95.0	655.1	3.5	0.0030	326.9	(2.54)		
C-RCCSD(T)+DKH2/C5Z	1492.52745	1.7783	92.1	656.6	3.8	0.0025	327.1	(2.35)		81

TABLE 4: Continued

method/basis set[a]	$-E$	r_e	D_e	ω_e	$\omega_e x_e$	α_e	ZPE	$\langle\mu\rangle$ (μ_{FF})[b]	Q_{Co}	T_e
				$^3\Sigma^-(d^8)$						
RCCSD(T)/4Z	1481.50214	1.7549	95.3							200
RCCSD(T)/5Z	1481.52554	1.7538	96.4							147
C-RCCSD(T)+DKH2/C5Z	1492.52680	1.7327	91.7	639.7	4.8	0.0035	318.6	(5.18)		224
				$^3\Delta(d^8)$						
RCCSD(T)/4Z	1481.49829	1.8049	92.9	581.2	2.3	0.0028	290.4			1045
RCCSD(T)/5Z	1481.52217	1.8025	94.3							887
C-RCCSD(T)+DKH2/C5Z	1492.52216	1.7847	88.7	597.8	3.9	0.0028	297.8	(5.15)		1242
				$^5\Sigma^-(s^1d^7)$						
RCCSD(T)/4Z	1481.48647	1.8263	85.5	617.3	3.1	0.0027	308.1	(3.21)		3639
RCCSD(T)/5Z	1481.50865	1.8245	85.8	620.5	3.7	0.0027	309.2	(3.17)		3854
C-RCCSD(T)+DKH2/C5Z	1492.50881	1.8225	80.4	620.7	4.1	0.0028	309.2			4172

[a] +Q and DKH2 refer to Davidson correction and to the second-order Douglas−Kroll−Hess scalar relativistic corrections. C- means that the semicore $3s^23p^6$ e^- have been correlated. [b] $\langle\mu\rangle$ was calculated as the expectation value and μ_{FF} through the finite field approach. [c] See text for the origin of this state. [d] Ref 25b. [e] Ref 26.

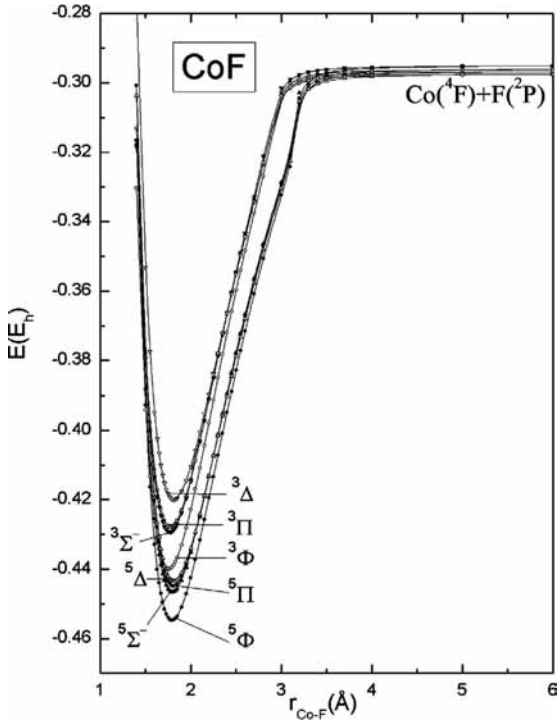

Figure 2. MRCI potential energy curves of the CoF molecule. All energies are shifted by +1481.0 E_h.

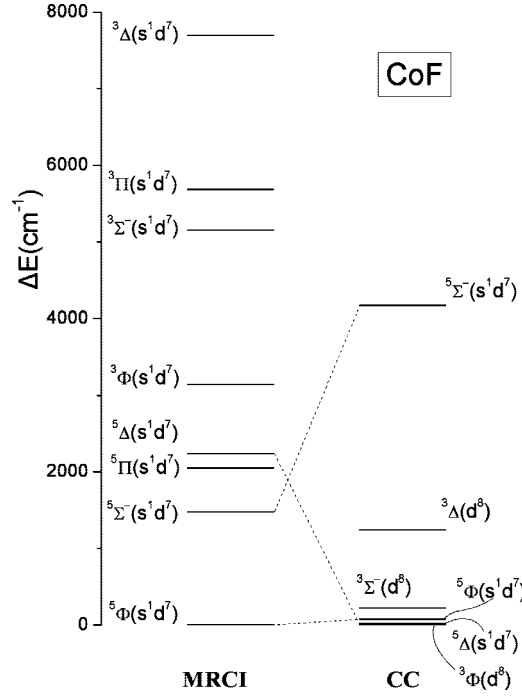

Figure 3. Relative energy diagram of eight and six CoF states calculated at the C-MRCI+DKH2+Q/C5Z and C-RCCSD(T)+DKH2/C5Z level, respectively.

$^3\Delta$;[25b] corresponding C-MRCI+DKH2+Q/C5Z r_e values are 1.738 ($^3\Phi$) and 1.797 ($^3\Delta$) Å, rather strengthening our conclusion as to the origin of these two triplets.

We discuss now the six states of s^1d^7 or d^8 origin but calculated at the CC level of theory (see Figure 3). At the highest CC level, C-RCCSD(T)+DKH2/C5Z, five states, $^3\Phi(d^8)$, $^5\Delta(s^1d^7)$, $^5\Phi(s^1d^7)$, $^3\Sigma^-(d^8)$, and $^3\Delta(d^8)$, are squeezed within 1237.8 cm^{-1} (or 5.64 mE_h), with the $^3\Phi(d^8)$ being formally the ground state. In particular, the first four states, $^3\Phi(d^8)$, $^5\Delta(s^1d^7)$, $^5\Phi(s^1d^7)$, and $^3\Sigma^-(d^8)$, are located within one mE_h (=220 cm^{-1}) interval, clearly degenerate within the accuracy of our calculations. Notice, first that at the highest CC level, the $^5\Delta(s^1d^7)-^5\Phi(s^1d^7)$ gap is −57 cm^{-1} (+463 cm^{-1} at the RCCSD(T)/4Z), at variance with the previous C-MRCI+DKH2+Q/C5Z result of 2241 cm^{-1}. We confess that we do not understand this discrepancy between the MRCI and CC results. On the other hand, the (CC) $^3\Delta(d^8)-^3\Phi(d^8)$ energy distance is 1237.8 cm^{-1}, as contrasted to the (MRCI) $^3\Delta(s^1d^7)-^3\Phi(s^1d^7)$ separation of 4559 cm^{-1}. As was argued before, this indicates that the experimental observation of the $^3\Delta - {}^3\Phi$ energy difference belongs to the s^1d^7 series. Calculated r_e values of the $^3\Phi(d^8)$ and $^3\Delta(d^8)$ states are of no help, being the same with the corresponding C-MRCI+DKH2+Q/C5Z values previously discussed. Notice as well that the $^5\Sigma^-(s^1d^7)$ is not calculated reliably at the CC level because its equilibrium composition changes drastically at the MRCI approach as compared to the ($\sqrt{(4/5)}$,$\sqrt{(1/5)}$) components of the Co^+ $^5F(s^1d^7)$ description.

The dilemma is now obvious: what is the ground state of CoF? In addition, what is the real $^5\Phi(s^1d^7)-^5\Delta(s^1d^7)$ splitting, −57 cm^{-1} (C-RCCSD(T)+DKH2/C5Z) or 2241 cm^{-1} (C-MRCI+DKH2+Q/C5Z)? Related to these questions is the binding energy (D_e) of the $^5\Phi(s^1d^7)$, which is calculated to be 97.9 and 92.1 kcal/mol at the highest MRCI and CC levels, respectively. We admit that we are at a weakness to answer these questions. We can only say that if the ground state is related to the $^5F(s^1d^7)$ of Co^+, it is $^5\Delta$ or $^5\Phi$, with the former more plausible at the CC level, or it is $^3\Phi$ if it is related to the $^3F(d^8)$ configuration of the Co^+ cation. Judging also from our

MRCI results, we are rather confident that if the in situ Co^+ belongs to the $s^1d^7(^3F)$ configuration, the $^3\Phi$ cannot be the lowest state, at variance with the conclusions of the Steimle's group.[28] Obviously, accurate experimental numbers or more extensive calculations are needed for both the triplet and quintet manifolds to resolve these questions. Particularly, the $^5\Phi-^5\Delta$ energy separation is a highly desired experimental result, of crucial importance to this conundrum.

Closing the discussion on CoF, our suggested binding energy, independent of the symmetry and origin of the ground state, is $D_e = 95 \pm 3$ kcal/mol, the higher, 98, and lower, 92 kcal/mol values, calculated at the MRCI and CC levels, respectively. Also, dipole moments of triplets or quintets originating from the s^1d^7 (^3F or ^5F) configuration of Co^+ are, on average, by 2 D smaller than those of the d^8 (^3F) descend; see Table 4.

C. NiF. Since 1953 when Krishnamurty[30] first observed the NiF diatomic, a large number of experimental publications followed,[31−48] indicating the strong interest of the scientific community on this system. A short chronological exposition of the salient experimental findings of NiF is in order at this point.

In 1981, Pinchemel,[32] by analyzing rotational transitions, proposed that the ground state of NiF is of $^2\Sigma^+$ symmetry, while five years later, Bai and Hilborn,[33] through chemiluminescence spectroscopy and by analogy with the isovalent species NiH, suggested an $X^2\Delta_{5/2}$ state. The same conclusion was reached later by Dufour et al.[35] through the rotational analysis of the $^2\Delta-^2\Pi$ transition. In 1994, Pinchemel's group,[37] after re-examining the data of ref 35, proposed that the ground state of NiF is of $^2\Pi_{3/2}$ symmetry with two $^2\Pi_{1/2}$ and $^2\Delta_{5/2}$ states lying 251 and 830 cm^{-1} higher. Continuing their insightful spectroscopic work, Dufour and Pinchemel[39] concluded that the state located 251 cm^{-1} above the $^2\Pi_{3/2}$ is not the $\Lambda + \Sigma = 1/2\ ^2\Pi$ component but a different electronic state of $^2\Sigma^+$ symmetry, although some doubts have been expressed lately[47] as to the symmetry of the latter. By now, it is rather established that the ground state of NiF is of $^2\Pi_{3/2}$ symmetry, with the $^2\Sigma^+$ and $^2\Delta_{5/2}$ states really close. Finally, the three most recent experimental bond dissociation energies reported in the literature give consistent values, namely, 101.5 ± 4.6,[34] 102.8 ± 2.5,[48] and very recently $D_0 = 104.4 \pm 1.4$ kcal/mol.[49] To the best of our knowledge, no experimental results are available for the quartet states.

We are aware of only one ab initio study of NiF by Zou and Liu.[50] These workers calculated the low-lying electronic states of NiX, X = F, Cl, Br, and I, at the CASPT2 level of theory, employing the DKH2 scalar relativistic atomic natural orbital basis sets developed by Roos et al.[51] For NiF in particular, the basis set used was [11s10p8d3f2g1h/$_{Ni}$5s4p3d2f1g/$_F$]. For 11 $^{2S+1}|\Lambda|$ and 26 $\Omega = \Lambda + \Sigma$ NiF states correlating diabatically to the three lowest states of Ni^+ (see below), Zou and Liu report T_e, r_e, and ω_e values.[50] Their results will be compared to ours later (Table 5).

Presently, we have studied 11 $^{2S+1}|\Lambda|$ states, the same as in ref 50, correlating adiabatically to the two lowest, practically degenerate, channels of Ni,[15b] [Ni(^{3}F;3d^{8}4s^2), Ni(^{3}D;3d^{9}4s^1)] + F(^{2}P). All states are highly ionic, tracing their diabatic ancestry to the three lowest states of Ni^+, ^{2}D(3d^9), ^{4}F(4s^{1}3d^8), and ^{2}F(4s^{1}3d^8), namely, {$^2\Sigma^+$, $^2\Pi$, $^2\Delta$}, {$^4\Sigma^-$, $^4\Pi$, $^4\Delta$, $^4\Phi$}, and {$^2\Sigma^-$, $^2\Pi$, $^2\Delta$, $^2\Phi$}, respectively. We were unable to calculate reliably the 3d^9 states ($^2\Sigma^+$, $^2\Pi$, $^2\Delta$) at the MRCI level. The 3d^9 doublets, including the $^4\Delta$ state, have been calculated at the CC level, while the remaining eight states, four quartets, and the four 4s^{1}3d^8 doublets have been calculated at the MRCI level. Obviously, this makes our comparison among the states difficult, the situation being similar to the previously discussed CoF molecule. For this reason, the 11 states studied are tagged as follows: $^2\Sigma^+(d^9)$, $^2\Pi(d^9)$, $^2\Delta(d^9)$, $^4\Sigma^-(s^1d^8)$, $^4\Pi(s^1d^8)$, $^4\Delta(s^1d^8)$, $^4\Phi(s^1d^8)$, $^2\Sigma^-(s^1d^8)$, $^2\Pi(s^1d^8)$, $^2\Delta(s^1d^8)$, and $^2\Phi(s^1d^8)$; see Table 5.

We discuss first the three d^9 doublets and the $^4\Delta(s^1d^8)$ state calculated at the CC level, followed by the s^1d^8 states' quartets and doublets calculated at the MRCI level. Figure 4 shows a relative energy diagram composed of two "disjoint" sets, CC, MRCI, and CASPT2 (ref 50). Notice that the location of $^4\Delta(s^1d^8)$ as calculated in both methods is arbitrarily positioned at the same energy separation in both CC and MRCI approaches. Figure 5 displays PECs of all s^1d^8 states, and Table 5 collects all numerical results on NiF.

***X*$^2\Pi(d^9)$, *A*$^2\Sigma^+(d^9)$, *and B*$^2\Delta(d^9)$.** The three states above, calculated only at the CC level, are located within a 2 kcal/mol interval. As the level of calculation increases from RCCSD(T)/4Z to C-RCCSD(T)+DKH2/C5Z, the order of the $^2\Pi(d^9)$ and $^2\Sigma^+(d^9)$ states changes: the $^2\Pi(d^9)$ becomes the lowest by just 101 cm^{-1} at the highest level, declared formally as the ground state. Certainly these two states are degenerate within the accuracy of our calculations. Experimentally, it seems rather certain that the ground state is of $^2\Pi_{3/2}$ symmetry (vide supra), being lower than the $^2\Sigma^+(d^9)$ state by 251.26 cm^{-1}.[47] Experimentally, the most recent dissociation energy is $D_0 = 104.4 \pm 1.4$ kcal/mol obtained by mass spectrometry.[49] At the C-RCCSD(T)/C5Z level, we calculate $D_e = 110.8$ kcal/mol, 1.9 kcal/mol higher than the RCCSD(T)/5Z value. However, scalar relativistic effects lower the binding energy by 7.8 (without core electrons) or 8.2 (including core electrons) kcal/mol (Table 5). Our final C-RCCSD(T)+DKH2/C5Z D_0 value with respect to Ni(^{3}F) + F(^{2}P) is $D_0 = 102.6 - ZPE - BSSE = 102.6 - 0.90 - 0.30$ kcal/mol $= 101.3$ kcal/mol, in very good agreement with experiment. The r_e value is also in excellent agreement with experiment, 1.7357 versus 1.73871 Å.[47] The CASPT2 bond distance and ω_e values of Zou and Liu[50] are similar to ours; these authors do not report other spectroscopic constants beyond r_e (B_e) and ω_e. In the $A^2\Sigma^+(d^9)$ state, the scalar relativistic effects lower the binding energy about 10 kcal/mol. The C-RCCSD(T)+DKH2/C5Z r_e value is calculated as 0.023 Å larger than the experimental value,[47] similar to the CASPT2 one.[50] However, the CASPT2 energy separation $A^2\Sigma^+(d^9)-X^2\Pi(d^9)$ is calculated to be 1801 cm^{-1}, as contrasted to an experimental value[47] of 251.26 cm^{-1} and our value of 101 cm^{-1}.

The discussion above can be repeated for the $B^2\Delta(d^9)$ state. The r_e and ω_e values are in very good agreement with experiment[47] at both the C-RCCSD(T)+DKH2/C5Z and CASPT2[50] levels; however, the T_e value of the latter is 1474 cm^{-1} as compared to 829.48 cm^{-1} of experiment ($^2\Delta_{5/2}-^2\Pi_{3/2}$) and our value of 756 cm^{-1}.

A comment is needed for the dipole moments of the d^9 doublets, all very close to 5 D, approximately 2 D higher than those of the s^1d^8 states' doublets, and quartets. This quite large and consistent difference is perhaps due to the more spherical distribution of the d^9 Ni^+ configuration as compared to s^1d^8; thus, the former approaches more its classical Coulombic value of 8 D, assuming a charge transfer of one electron from Ni to F and a bond distance of 1.7 Å. The same effect was observed in CrF ($X^6\Sigma^+$)[1] and CuF ($X^1\Sigma^+$) (see below).

$^4\Delta(s^1d^8)$. This is the only state that we were able to calculate with both the MRCI and CC methods with consistent results due to the fact that it is of strictly single reference character (see below).

TABLE 5: Total Energies E (E_h), Equilibrium Bond Distances r_e (Å), Dissociation Energies with Respect to the Ground-State Atoms D_e (kcal/mol), Harmonic and Anharmonic Frequencies ω_e, $\omega_e x_e$ (cm^{-1}), Rotational−Vibration Constants α_e (cm^{-1}), Zero Point Energies ZPE (cm^{-1}), Dipole Moments μ_e (D), Mulliken Charges Q_{Ni}, and Energy Separations T_e (cm^{-1}) of NiF

method/basis set[a]	−E	r_e	D_e	ω_e	$\omega_e x_e$	α_e	ZPE	$\langle\mu\rangle$ (μ_{FF})[b]	Q_{Ni}	T_e
RCCSD(T) Results										
$X^2\Pi(d^9)$										
RCCSD(T)/4Z	1607.05079	1.7564	107.9	611.5	2.7	0.0033	305.6	(5.41)	0.84	0.0
RCCSD(T)/5Z	1607.07943	1.7552	108.9	611.0	2.8	0.0036	305.4	(5.41)	0.84	0.0
RCCSD(T)+DKH2/5Z	1619.35914	1.7322	101.1	637.0	2.6	0.0035	318.5	(5.11)		0.0
C-RCCSD(T)/C5Z	1607.56362	1.7588	110.8	610.4	3.4	0.0035	304.7	(5.40)		0.0
C-RCCSD(T)+DKH2/C5Z	1619.84429	1.7357	102.6	634.2	3.6	0.0034	316.5	(5.20)		0.0
CASPT2[c]		1.728		643						0.0
expt.		1.73871[d]	101.5 ± 4.6[e] 102.8 ± 2.5[f] 104.4 ± 1.4[g]	644 ($\Delta G_{1/2}$)[d]						
$A^2\Sigma^+(d^9)$										
RCCSD(T)/4Z	1607.05214	1.7754	108.8	611.2	2.5	0.0029	305.3	(5.48)	0.85	−296
RCCSD(T)/5Z	1607.08100	1.7738	109.9	613.4	3.4	0.0030	305.9	(5.48)	0.84	−345
RCCSD(T)+DKH2/5Z	1619.35757	1.7598	100.1	620.8	2.8	0.0030	309.9	(5.30)		345
C-RCCSD(T)/C5Z	1607.56600	1.7745	112.3					(5.47)		−522
C-RCCSD(T)+DKH2/C5Z	1619.84383	1.7607	102.4	622.4	2.8	0.0030	310.8	(5.30)		101
CASPT2[c]		1.766		626						1801
expt.[d]		1.73814		607 ($\Delta G_{1/2}$)						251.26[h]
$B^2\Delta(d^9)$										
RCCSD(T)/4Z	1607.04611	1.7605	105.0	628.0	4.0	0.0033	313.0	(5.21)	0.83	1027
RCCSD(T)/5Z	1607.07471	1.7596	106.0	627.3	4.2	0.0034	312.6	(5.23)	0.83	1036
RCCSD(T)+DKH2/5Z	1619.35658	1.7373	99.5	660.1	4.0	0.0035	329.3	(4.87)		562
C-RCCSD(T)/C5Z	1607.55807	1.7641	107.3					(5.28)		1218
C-RCCSD(T)+DKH2/C5Z	1619.84081	1.7408	100.5	652.8	4.3	0.0036	325.5	(4.95)		765
CASPT2[c]		1.737		646						1474
expt.[d]		1.73779		653 ($\Delta G_{1/2}$)						829.48[i]
$^4\Delta(s^1d^8)$										
RCCSD(T)/4Z	1607.02402	1.7832	91.1	651.0	3.3	0.0028	324.8	(2.80)	0.71	5875
C-RCCSD(T)+DKH2/C5Z	1619.81972	1.7784	87.2	654.0	3.6	0.0027	326.2	(3.01)		5394
CASPT2[c]		1.774		668						5915
$^4\Sigma^-(s^1d^8)$										
RCCSD(T)/4Z	1607.02134	1.7622	89.4					(2.65)	0.70	6464
C-RCCSD(T)+DKH2/C5Z	1619.81724	1.7502	87.8					(2.50)		5937
CASPT2[c]		1.759		660						5572
MRCI Results[j]										
$^4\Pi(s^1d^8)$										
MRCI/4Z	1606.96010	1.7741	90.6	650.6	3.3	0.0028	324.6	2.73 (2.80)	0.65	$+x$
MRCI+Q	1607.0059	1.769	92.3	652.0	3.3	0.0029	325.2			
MRCI/5Z	1606.98515	1.7728	90.9	649.7	2.8	0.0029	324.5	2.70 (2.80)	0.75	
MRCI+Q	1607.0322	1.768	92.8	653.0	3.5	0.0029	325.8			
MRCI+DKH2/5Z	1619.27137	1.7682	87.9	650.9	3.0	0.0031	325.1	2.71 (2.80)	0.74	
MRCI+DKH2+Q	1619.3191	1.763	89.7	652.1	2.2	0.0029	326.0			
C-MRCI/C5Z	1607.40262	1.7732	89.5	650.9	2.9	0.0029	325.1	2.76 (2.86)	0.81	
C-MRCI+Q	1607.4936	1.768	92.4	652.2	2.9	0.0031	325.8			
C-MRCI+DKH2/C5Z	1619.68983	1.7686	86.5	651.9	3.2	0.0031	325.4	2.76 (2.86)	0.80	
C-MRCI+DKH2+Q	1619.7816	1.763	89.3	656.3	3.4	0.0029	327.4			
CASPT2[c]		1.758		646						5449[k]
$^4\Delta(s^1d^8)$										
MRCI/4Z	1606.95860	1.7878	89.4	651.6	3.3	0.0028	325.2	2.90 (3.05)	0.66	$x + 329$
MRCI+Q	1607.0035	1.786	90.5	650.8	3.4	0.0028	324.6			524
MRCI/5Z	1606.98370	1.7863	89.7	649.9	2.7	0.0029	324.7	2.86 (3.05)	0.76	317
MRCI+Q	1607.0299	1.785	90.9	653.1	3.8	0.0028	325.6			509
C-MRCI+DKH2/C5Z	1619.68774	1.7826	85.2	652.5	3.2	0.0031	325.8	2.91 (3.05)	0.80	459
C-MRCI+DKH2+Q	1619.7786	1.781	87.4	656.5	4.1	0.0028	327.2			659
CASPT2[c]		1.774		668						466[k]
$^4\Sigma^-(s^1d^8)$										
MRCI/4Z	1606.95612	1.7824	88.6	639.7	3.2	0.0028	319.2	2.78 (2.86)	0.66	$x + 873$
MRCI+Q	1607.0025	1.776	90.7	642.5	3.3	0.0028	320.6			749
C-MRCI+DKH2/C5Z	1619.68675	1.7752	84.6	641.2	2.6	0.0028	320.3	2.82 (2.92)	0.81	676
C-MRCI+DKH2+Q	1619.7791	1.768	87.6	645.1	3.1	0.0030	322.0			560
CASPT2[c]		1.759		660						123[k]
$^2\Delta(s^1d^8)$										
MRCI/4Z	1606.95182	1.7460	85.1	676.2	3.5	0.0029	337.3	3.02 (3.94)	0.62	$x + 1817$

TABLE 5: Continued

method/basis set[a]	$-E$	r_e	D_e	ω_e	$\omega_e x_e$	α_e	ZPE	$\langle\mu\rangle$ (μ_{FF})[b]	Q_{Co}	T_e
MRCI+Q	1606.9996	1.739	88.0	679.9	3.5	0.0029	339.2			1382
C-MRCI+DKH2/C5Z	1619.67903	1.7407	79.7	676.3	2.0	0.0028	338.3	2.97 (3.81)	0.79	2370
C-MRCI+DKH2+Q	1619.7727	1.733	83.7	681.8	3.3	0.0030	340.3			1966
CASPT2[c]		1.814		598						8316[k]
				$^2\Pi(s^1d^8)$						
MRCI/4Z	1606.94664	1.7514	82.2	655.2	3.3	0.0028	326.8	2.67 (3.24)	0.61	x + 2955
MRCI+Q	1606.9945	1.742	85.2	657.4	3.3	0.0029	328.0			2493
C-MRCI+DKH2/C5Z	1619.67434	1.7463	76.8	657.5	2.7	0.0029	328.4	2.64 (3.18)	0.79	3398
C-MRCI+DKH2+Q	1619.7681	1.737	80.8	659.6	2.3	0.0028	329.7			2965
CASPT2[c]		1.788		633						6233[k]
expt.[d]		1.79154 (r_0)		619						11096.05[l]
				$^4\Phi(s^1d^8)$						
MRCI/4Z	1606.94582	1.8085	81.7	619.2	3.2	0.0028	309.0	3.01 (3.18)	0.67	x + 3134
MRCI+Q	1606.9916	1.803	83.4	620.5	3.1	0.0028	309.7			3144
C-MRCI+DKH2/C5Z	1619.67576	1.8000	77.7	624.0	4.0	0.0028	310.8	3.00 (3.18)	0.80	3087
C-MRCI+DKH2+Q/C5Z	1619.7674	1.795	80.3	625.1	3.2	0.0028	311.8			3117
CASPT2[c]		1.791		619						3376[k]
				$^2\Sigma^-(s^1d^8)$						
MRCI/4Z	1606.93721	1.7867	76.7	640.1	3.2	0.0028	319.5	2.81 (2.67)	0.64	x + 5025
MRCI+Q	1606.9851	1.779	79.8	643.0	3.2	0.0028	320.8			4573
C-MRCI+DKH2/C5Z	1619.66574	1.7796	71.4	641.3	2.9	0.0032	320.3	2.83 (2.67)	0.80	5285
C-MRCI+DKH2+Q	1619.7595	1.773	75.4	647.8	3.9	0.0029	322.8			4850
CASPT2[c]		1.756		622						5068[k]
				$^2\Phi(s^1d^8)$						
MRCI/4Z	1606.92887	1.8087	71.0	623.2	3.2	0.0028	311.0	2.80 (2.92)	0.64	x + 6856
MRCI+Q	1606.9756	1.804	73.4	624.0	3.1	0.0028	311.3			6646
C-MRCI+DKH2/C5Z	1619.65697	1.800	65.9	626.9	3.4	0.0028	312.7	2.78 (2.80)	0.79	7210
C-MRCI+DKH2+Q	1619.7496	1.796	69.1	628.1	3.3	0.0028	313.3			7041
CASPT2[c]		1.793		633						7310[k]
expt.[d]		1.79110		621						12567.76[m]

[a] +Q refers to the Davidson correction and DKH2 to second-order Douglas−Kroll−Hess scalar relativistic corrections. C- means that the Ni semicore $3s^23p^6$ electrons have been correlated. [b] $\langle\mu\rangle$ was calculated as an expectation value and μ_{FF} through the finite field approach. [c] Ref 50; see text. [d] Ref 47. [e] Ref 34. [f] Ref 48. [g] Ref 49. [h] Ref 47; this energy separation refers to $X^2\Pi_{3/2}-{}^2\Sigma^+$. [i] Ref 47; this energy separation refers to $X^2\Pi_{3/2}-{}^2\Delta_{5/2}$. [j] The $+x$ means that we were unable to locate the T_e value with respect to the $X^2\Pi$ state. [k] With respect to the $^4\Pi(s^1d^8)$ of ref 50. [l] $[11.1]^2\Pi_{3/2} \leftarrow X^2\Pi_{3/2}$ transition; ref 47. [m] $[12.0]^2\Phi_{7/2} \leftarrow X^2\Pi_{3/2}$ transition; ref 47.

With respect to the $X^2\Pi(d^9)$ state, the $^4\Delta(s^1d^8)$ is located 5394 cm^{-1} higher as obtained at the C-RCCSD(T)+DKH2/C5Z level; the corresponding number is 5915 cm^{-1} calculated by the CASPT2 approach.[50] As can be seen from Table 5, r_e, D_e, and ω_e values are practically identical at the highest CC and MRCI levels of theory. Observe however that we do not know the absolute location of the s^1d^8 quartets and doublets calculated through the MRCI methodology due to our inability to calculate by this method the d^9 doublets; therefore, the lowest $^4\Pi(s^1d^8)$ state is arbitrarily considered as $+x$ higher from the $X^2\Pi(d^9)$ state; see Figure 4.

$^4\Pi(s^1d^8)$, $^4\Sigma^-(s^1d^8)$, $^4\Delta(s^1d^8)$, $^2\Delta(s^1d^8)$, $^2\Pi(s^1d^8)$, $^4\Phi(s^1d^8)$, $^2\Sigma^-(s^1d^8)$, and $^2\Phi(s^1d^8)$. The MRCI/4Z PECs of all of the s^1d^8 quartets and doublets are displayed in Figure 5, while Figure 4 shows their relative position. With the exception of the $^2\Pi(s^1d^8)$ and $^2\Delta(s^1d^8)$ states (see below), the ordering of the rest of the states is pretty similar to the one obtained in ref 50. In what follows, we first describe, in short, the quartets and then the doublets.

First, we can estimate the $+x$ value from the relation $x \approx D_e(X^2\Pi)/CC - D_e(^4\Pi)/MRCI$ because both D_e's are calculated with respect to the ground-state atoms, $Ni(^3F) + F(^2P)$, and assuming that our D_e values are close to reality, as is indeed the case for the $X^2\Pi(d^9)$. Thus, $x \approx 102.6 - 89.2 = 13.3$ kcal/mol, or 4652 cm^{-1}, as compared to the corresponding T_e = 5449 cm^{-1} obtained in ref 50. Obviously, experimental results "connecting" doublets and quartets are highly desirable.

The first three s^1d^8 quartets, $^4\Pi$, $^4\Sigma^-$, and $^4\Delta$, are lying within an energy range of 659 cm^{-1} at the C-MRCI+DKH2+Q/C5Z level; see Figure 4 and Table 5. Following the same convention as before, the leading CASSCF CFs are

$$|^4\Pi\rangle_{B_1} \approx |(0.75)(3\sigma^1 4\sigma^1 2\pi_x^1 2\pi_y^2 1\delta_+^2 1\delta_-^2) + (0.46)(3\sigma^2 4\sigma^1)(2\pi_x^1 2\pi_y^2 1\delta_+^1 1\delta_-^2 + 2\pi_x^2 2\pi_y^1 1\delta_+^2 1\delta_-^1)\rangle$$

$$|^4\Delta\rangle_{A_2} = 0.997|3\sigma^1 4\sigma^1 2\pi_x^2 2\pi_y^2 1\delta_+^2 1\delta_-^1\rangle$$

$$|^4\Sigma^-\rangle \approx |(3\sigma^2 4\sigma^1)[(0.94)2\pi_x^1 2\pi_y^1 1\delta_+^2 1\delta_-^2 + (0.34)2\pi_x^2 2\pi_y^2 1\delta_+^1 1\delta_-^1]\rangle$$

As we increase the level of calculation from MRCI/4Z to C-MRCI+DKH2+Q, the energy difference between the $^4\Delta$ and $^4\Sigma^-$ diminishes, with the latter becoming finally the lowest by a mere 99 cm^{-1} after adding the Davidson correction. Of course, for the current calculations, the $^4\Delta$ and $^4\Sigma^-$ are considered degenerate. Although the ordering of these first three quartets is predicted to be the same at the CASPT2 level,[50] the $^4\Pi-{}^4\Sigma^-$ and $^4\Delta-{}^4\Sigma^-$ splittings are somehow different, 123 and 343 cm^{-1}, respectively, as compared to 560 and 99 cm^{-1} at the highest MRCI level. In addition, r_e and ω_e values are very similar in both the CASPT2 and C-MRCI+DKH2+Q/C5Z methods (Table 5).

The $^4\Phi(s^1d^8)$ state is composed of two equally weighted CASSCF configurations, namely

$$|^4\Phi\rangle_{B_1} = \sqrt{1/2}|(3\sigma^2 4\sigma^1)(2\pi_x^1 2\pi_y^2 1\delta_+^1 1\delta_-^2 - 2\pi_x^2 2\pi_y^1 1\delta_+^2 1\delta_-^1)\rangle$$

and is well separated from the $^4\Pi$ state, $\Delta E(^4\Phi-{}^4\Pi) = 3117$ cm^{-1} at the highest MRCI level, predicted identical to the

CASPT2 value of 3376 cm^{-1}. The same is true for the r_e and ω_e values, as can be seen from Table 5.

We turn now to the four s^1d^8 doublets, whose main CASSCF CFs are given below

$$|^2\Delta\rangle_{A2} \approx |2\pi_x^2 2\pi_y^2 1\delta_+^2[(0.62)3\sigma^2 1\delta_-^1 + (0.51)3\sigma^1 4\bar{\sigma}^1 1\delta_-^1 - (0.46)3\sigma^1 4\sigma^1 1\bar{\delta}_-^1 - (0.38)4\sigma^2 1\delta_-^1]\rangle$$

$$|^2\Pi\rangle_{B1} \approx |[(0.61)3\sigma^1 4\bar{\sigma}^1 + (0.25)3\sigma^2]2\pi_x^1 2\pi_y^2 1\delta_+^2 1\delta_-^2 + 3\sigma^2 4\sigma^1 2\pi_x^2 1\delta_+^2[(0.39)2\bar{\pi}_y^1 1\delta_-^1 + (0.23)2\pi_y^1 1\bar{\delta}_-^1] + [(0.39)3\sigma^2 4\bar{\sigma}^1 2\pi_x^1 1\delta_+^1 - (0.36)3\sigma^1 4\sigma^1 2\bar{\pi}_x^1 1\delta_+^2 - (0.22)3\sigma^2 4\sigma^1 2\bar{\pi}_x^1 1\delta_+^1]2\pi_y^2 1\delta_-^1\rangle$$

$$|^2\Sigma^-\rangle \approx |3\sigma^2 4\sigma^1 1\delta_+^2 1\delta_-^2[(0.75)2\bar{\pi}_x^1 2\bar{\pi}_y^1 + (0.43)2\pi_x^1 2\bar{\pi}_y^1] + (0.30)3\sigma^1 4\sigma^2 2\bar{\pi}_x^1 2\pi_y^1 1\delta_+^2 1\delta_-^2 + (0.28)3\sigma^2 4\bar{\sigma}^1 2\pi_x^2 2\pi_y^2 1\delta_+^1 1\delta_-^1\rangle$$

$$|^2\Phi\rangle_{B1} \approx |(0.61)(3\sigma^2 4\bar{\sigma}^1 2\pi_x^1 2\pi_y^2 1\delta_+^1 1\delta_-^2 - 3\sigma^2 4\sigma^1 2\pi_x^2 2\bar{\pi}_y^1 1\delta_+^2 1\delta_-^1) - (0.35)3\sigma^2 4\sigma^1(2\pi_x^2 2\pi_y^1 1\delta_+^2 1\bar{\delta}_-^1 + 2\bar{\pi}^1 2\pi_y^2 1\delta_+^1 1\delta_-^2)\rangle$$

all of them of intense multireference character and correlating diabatically to the second excited state of $Ni^+(^2F)$.

The C-MRCI+DKH2+Q/C5Z T_e values of the $^2\Delta$, $^2\Pi$, $^2\Sigma^-$, and $^2\Phi$ with respect to the $^4\Pi$ state are 1966, 2965, 4850, and 7041 cm^{-1}, respectively. The corresponding ordering of Zou and Liu[50] is 8316, 6233, 5068, and 7310 cm^{-1}, a different ordering from ours, the lowest state being the $^2\Sigma^-$ followed by the $^2\Pi$, $^2\Phi$, and $^2\Delta$. Near-infrared experimental results[47] vindicate the Zou and Liu CASPT2 numbers. Specifically, the T_0 experimental values are 11096.05 and 12008.92 cm^{-1} for the $^2\Pi_{3/2}$ and $^2\Phi_{7/2}$, respectively, and are of s^1d^8 character, as suggested by the experimentalists.[47] The corresponding numbers of Zou and Liu with respect to the X state are 11682 and 12759 cm^{-1}, in good agreement with experiment. Note that the relative location of the $^2\Phi(s^1d^8)$ is predicted correctly in the present work as compared with that of the CASPT2 work of ref 50, 7041 versus 7310 cm^{-1}, and the experimental r_e and ω_e values (vide supra). The problem seems to be the $^2\Pi(s^1d^8)$ and the $^2\Delta(s^1d^8)$ states, which are down shifted by about 3000 and 6000 cm^{-1}, respectively, at the C-MRCI+DKH2+Q/C5Z level; see Figure 4. This problem is related to the failure of the MRCI to cope with the d^9 ($X^2\Pi$, $A^2\Sigma^+$, $B^2\Delta$) and the s^1d^8 (Δ, Π) doublets.

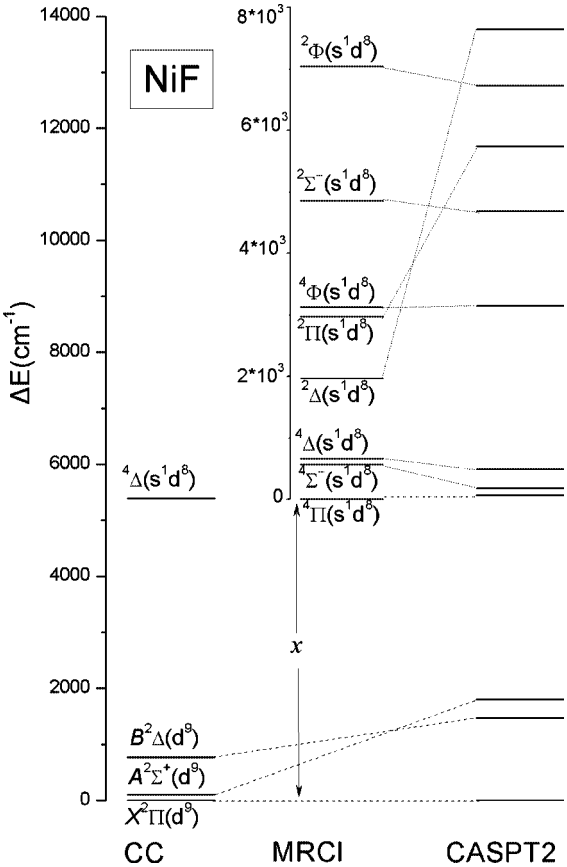

Figure 4. Relative energy diagram of 4, 8, and 11 NiF states calculated at the C-RCCSD(T)+DKH2/C5Z, C-MRCI+DKH2+Q/C5Z, and CASPT2 (ref 50) levels, respectively.

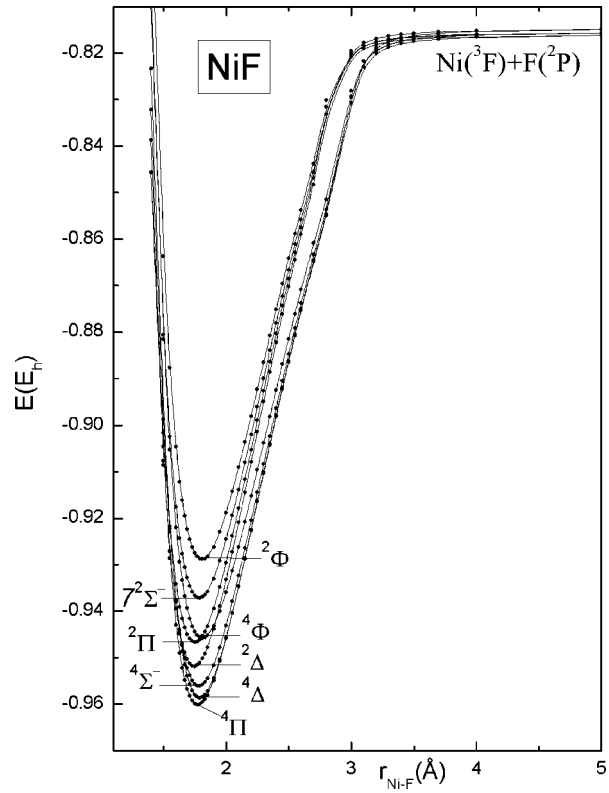

Figure 5. MRCI potential energy curves of the $Ni^+(s^1d^8)F^-$ molecule. All energies areshifted by +1606.0 E_h.

Finally, we would like to mention that all states of NiF examined presently are quite ionic, with a charge transfer of 0.7−0.8 e^- from Ni to F. The avoided crossings with the Ni^+F^- states at the MRCI/4Z level shown in Figure 5 are around 3 Å, corresponding to a charge transfer of ~0.9 e^- as obtained from $q = [r_c(IE - EA)]^{1/2}$ where $r_c \approx 3$ Å.

D. CuF. It is interesting that the first emission spectrum of CuF was observed by Robert S. Mulliken as early as 1925.[52] Since then, we are aware of at least 22 experimental spectroscopic works on CuF.[49,53−73] The most recent and pertinent experimental results will be contrasted with ours later on.

A variety of theoretical publications exists in the literature,[74−82] with the first one published in 1982 by Dufour et al.[74] at the Hartree−Fock level. The most recent and comprehensive work is that of Guinchemerre et al., who examined the halides of coinage metals, MX, M = Cu, Ag, and Au and X = F, Cl, and Br.[82] These workers performed multireference and coupled-

cluster calculations using scalar relativistic effective core potentials (ECP) for both M and X, supplemented with valence basis sets. In particular, for the CuF molecule, they examined the seven lowest states around equilibrium at the MRCI, CCSD(T), and EOM-CCSD (equation of motion CC), in conjunction with ECP + [7s6p4d3f2g/$_{Cu}$6s6p3d2f/$_{F}$].[82] Their findings are compared with the current results in Table 6.

The ground state of Cu is ^{2}S($4s^13d^{10}$), with the first excited state of ^{2}D($4s^23d^9$) symmetry located above the ^{2}S by 12019.7 cm^{-1} (M_J averaged).[15b] At the C-RCCSD(T)+DKH2/CBP level, the ^{2}D−^{2}S splitting is calculated to be 11654 cm^{-1}. The corresponding MRCI(+Q)/4Z number obtained from the asymptotes of the PECs (Figure 6) is 7328 (13111) cm^{-1}.

As in the previously reported fluorides, the states of CuF can be thought of as arising from the low terms of Cu^+ in the field of F^-. Presently, we have studied seven low-lying states of CuF related to the first three terms of Cu^+, that is, ^{1}S($3d^{10}$), ^{3}D($4s^13d^9$), and ^{1}D($4s^13d^9$). The experimental energy separations ^{3}D−^{1}S and ^{1}D−^{1}S are (M_J averaged) 2.808 and 3.256 eV, respectively;[15b] theoretical MRCI and CC results on these splittings are given in Table 2. The seven $^{2S+1}|\Lambda|$ states emanating from these atomic states are [$^1\Sigma^+$], [$^3\Sigma^+$, $^3\Pi$, $^3\Delta$], and [$^1\Sigma^+$, $^1\Pi$, $^1\Delta$], respectively.

All seven states have been calculated by the MRCI method. The RCCSD(T) approach was applied to $X^1\Sigma^+$, $a^3\Sigma^+$, $b^3\Pi$, and $c^3\Delta$; the last three singlets $^1\Sigma^+$, $^1\Pi$, and $^1\Delta$ related to $Cu^+(4s^23d^9)$ are not accessible by the CC method. This caused some difficulties in positioning the seven states relative to the ground state (vide infra). It should also be stressed that we encountered a variety of problems in constructing full adiabatic MRCI curves, caused by the "intricate" configuration $4s^13d^{10}$ of Cu and the interplay between the $3d^{10}$ and $4s^13d^9$ configuration of Cu^+ entangled in the excited states.

MRCI/4Z PECs along with a relative energy level diagram are given in Figure 6, whereas Table 6 covers all of our numerical results, including experimental values and theoretical results from ref 82.

***X*$^1\Sigma^+$.** The ground state of CuF, of $^1\Sigma^+$ symmetry, is well separated from the rest of the states correlating adiabatically to Cu(^{2}S;$4s^13d^{10}$) + F(^{2}P) and diabatically to Cu^+(^{1}S;$3d^{10}$) + F^-(^{1}S), and as expected, it is very ionic, with a charge transfer of 0.8−0.9 e$^-$ from Cu to F. As the level of calculation increases, the bond length converges to the experimental value, somehow irregularly at the MRCI level, but monotonically at the CC level. The C-RCCSD(T)+DKH2/C5Z r_e is 1.7479 Å, in excellent agreement with experiment, the latter being shorter by 0.003 Å; Table 6. Scalar relativistic effects play a role in bringing the calculated bond distance in agreement with experiment, shortening the r_e by about 0.025 Å in both MRCI and CC methods. The binding energy as seen from Table 6 is in good agreement with experiment at all levels of theory. At the highest CC level, we obtain D_e = 98.2 kcal/mol, or D_0 = D_e − ZPE − BSSE = 98.2 kcal/mol − 307.14 cm^{-1} − 0.3 kcal/mol = 97.0 kcal/mol, in excellent agreement with the experimental chemiluminescence value, D_0 = 98.07 kcal/mol,[73] but differing by −5 kcal/mol from the mass spectrometric value.[49]

Relativistic effects reduce the dipole moment by 0.3 D in both MRCI and CC methods. The C-MRCI+DKH2+Q [C-RCCSD(T)]/C5Z μ_{FF} value is 5.59 [5.33] D, as contrasted to an experimental value of 5.7$_7$ D.[83] Trusting more the CC results for this completely single reference $X^1\Sigma^+$ CuF state, we express some doubts for the experimental value of the dipole moment; perhaps, it is overestimated by 0.3 D.

***a*$^3\Sigma^+$, *b*$^3\Pi$, *and c*$^3\Delta$.** The three triplets above have been calculated at the "simple" MRCI+Q/4Z level and at the RCCSD(T) and C-RCCSD(T)+DKH2/C5Z levels. Extending the MRCI calculations to a higher level was prohibitively costly. To give just an example, the C-MRCI+DKH2/C5Z internally contracted expansion of the $B^1\Pi$ state (one of the singlets not accessible at CC) contains 96 × 10^6 CFs.

The leading equilibrium CASSCF CFs of the triplets are $|a^3\Sigma^+\rangle = 0.995|3\sigma^14\sigma^12\pi_x^22\pi_y^21\delta_+^21\delta_-^2\rangle$, $|b^3\Pi\rangle_{B_1} = 0.995|3\sigma^24\sigma^12\pi_x^12\pi_y^21\delta_+^21\delta_-^2\rangle$, and $|c^3\Delta\rangle_{A_1} = 0.994|3\sigma^24\sigma^12\pi_x^22\pi_y^21\delta_+^11\delta_-^2\rangle$, clearly of single reference character.

The $a^3\Sigma^+$ state is the first excited state, 14580.5 cm^{-1} above the $X^1\Sigma^+$ state,[60] in excellent agreement with our C-RCCSD(T)+DKH2/C5Z T_e value. The MRCI+Q result can also be considered to be in good aggreement, but the uncorrected with respect to +Q T_e = 10370 cm^{-1} is problematic due to the severe nonextensivity of the MRCI method applied to a system of 18 correlated electrons; see Table 6. The $a^3\Sigma^+$ is the only one of the six excited states studied which correlates adiabatically to the ground-state neutral fragments, Cu(^{2}S) + F(^{2}P; M_L = 0). With respect to Cu(^{2}S) + F(^{2}P), the C-RCCSD(T)+DKH2/C5Z (MRCI/4Z) dissociation energy is D_e = 56.1 (54.0) kcal/mol. Finally, the parameters r_e, ω_e, and $\omega_e x_e$ are in remarkably good agreement with experiment in both the MRCI+Q and CC methods, considering the complexity of the system.

The next state, $b^3\Pi$, correlates adiabatically to Cu(^{2}D; M_L = ±1) + F(^{2}P; M_L = 0) or diabatically to Cu^+(^{3}D; M_L = ±1) + F^-(^{1}S). Experimentally, it is located 17543.2 cm^{-1} above the X state,[66] in complete agreement with the T_e = 17596 cm^{-1} C-RCCSD(T)+DKH2/C5Z value. In this case, the MRCI T_e can be considered as acceptable, but the +Q corrected value is overestimated by 2500 cm^{-1}. The r_e, ω_e, and $\omega_e x_e$ C-RCCSD(T)+DKH2/C5Z numbers are in excellent agreement with the experiment,[66] whereas the D_e = 81.2 kcal/mol value with respect to the adiabatic terms should be quite accurate.

The higher of the triplets studied is of $^3\Delta$ symmetry and correlates adiabatically to Cu(^{2}D; M_L = ±2) + F(^{2}P; M_L = 0) or diabatically to Cu^+(^{3}D; M_L = ±2) + F^-(^{1}S), with an experimental energy separation $c^3\Delta-X^1\Sigma^+$ of 22639 cm^{-1},[60] the only experimental datum available (Table 6).

At the C-RCCSD(T)+DKH2/C5Z (MRCI+Q/4Z) level, $T_e(c^3\Delta-X^1\Sigma^+)$ = 21436 (20667) cm^{-1}, differing by 1200 (2200) cm^{-1} from the experimental value of 22639 cm^{-1}.[60] The rest of the calculated constants, r_e, ω_e, ZPE, and μ_e are calculated quite consistently in both C-RCCSD(T)+DKH2/C5Z and MRCI+Q/4Z methods.

***A*$^1\Sigma^+$, *B*$^1\Pi$, *and C*$^1\Delta$.** As was discussed previously in this section, the symmetry of the singlets above cannot be handled by a single reference method; therefore, these states were calculated by the MRCI method only. Their main CASSCF equilibrium CFs are the following

$$|A^1\Sigma^+\rangle \approx |[(0.90)3\sigma^14\bar{\sigma}^1 - (0.30)3\sigma^2]2\pi_x^22\pi_y^21\delta_+^21\delta_-^2\rangle$$

$$|B^1\Pi\rangle_{B1} = 0.995|3\sigma^24\sigma^12\bar{\pi}_x^12\bar{\pi}_y^21\delta_+^21\delta_-^2\rangle$$

$$|C^1\Delta\rangle_{A1} = 0.99|3\sigma^24\bar{\sigma}^12\pi_x^22\pi_y^21\delta_+^11\delta_-^2\rangle$$

They correlate adiabatically to Cu(^{2}D; M_L = 0, ±1, ±2) + F(^{2}P; M_L = 0) or diabatically to Cu^+(^{1}D; M_L = 0, ±1, ±2) + F^-(^{1}S); see Figure 6. Experimental results are available for the $A^1\Sigma^+$ and $B^1\Pi$ states but not for the $C^1\Delta$.

Concerning the $A^1\Sigma^+$ state, as we increase the level of the MRCI calculation, we move away from the experimental r_e and $T_e(A^1\Sigma^+-X^1\Sigma^+)$ values, and our best results are obtained at the simple MRCI+Q level, namely, r_e = 1.771 Å, and T_e = 18069

TABLE 6: Total Energies E (E_h), Equilibrium Bond Distances r_e (Å), Dissociation Energies with Respect to the Ground-State Atoms D_e (kcal/mol), Harmonic and Anharmonic Frequencies ω_e, $\omega_e x_e$ (cm^{-1}), Rotational−Vibration Constants α_e (cm^{-1}), Zero Point Energies ZPE (cm^{-1}), Dipole Moments μ (D), Mulliken Charges Q_{Cu}, and Energy Separations T_e (cm^{-1}) of CuF

method/basis set[a]	$-E$	r_e	D_e	ω_e	$\omega_e x_e$	α_e	ZPE	$\langle\mu\rangle$ (μ_{FF})[b]	Q_{Cu}	T_e
				$X^1\Sigma^+$						
MRCI/4Z	1739.16329	1.7524	95.1	610.5	4.1	0.0033	304.4	5.92 (5.88)	0.75	0.0
MRCI+Q	1739.2326	1.769	94.1	587.5	4.0	0.0033	292.7			0.0
MRCI/5Z	1739.19157	1.7519	95.2	607.2	3.0	0.0034	303.3	5.93 (5.92)	0.76	0.0
MRCI+Q	1739.2621	1.768	94.5	585.2	3.2	0.0033	292.1			0.0
MRCI+DKH2/5Z	1753.44454	1.7259	96.2	643.4	4.8	0.0036	320.5	5.64 (5.57)	0.75	0.0
MRCI+DKH2+Q	1753.5137	1.739	94.2	619.1	5.1	0.0035	308.1			0.0
C-MRCI+DKH2/C5Z	1753.86250	1.7235	95.7					5.67 (5.59)	0.83	0.0
C-MRCI+DKH2+Q	1753.9755	1.737	94.1	619.5	4.5	0.0034	308.5			0.0
RCCSD(T)/4Z	1739.26428	1.7691	99.0	597.9	2.8	0.0031	298.5	(5.58)	0.83	0.0
RCCSD(T)/5Z	1739.29644	1.7674	99.5	601.2	4.1	0.0032	299.2	(5.56)	0.84	0.0
RCCSD(T)+DKH2/5Z	1753.54855	1.7445	99.1	619.1	3.5	0.0034	308.8	(5.31)	0.83	0.0
C-RCCSD(T)/C5Z	1739.78188	1.7706	98.7	598.2	2.9	0.0030	298.6	(5.57)	0.90	0.0
C-RCCSD(T)+DKH2/C5Z	1754.03543	1.7479	98.2	616.9	3.8	0.0034	307.4	(5.33)	0.89	0.0
MRCI[c]		1.73		691.2	5.24			5.80		0.0
CCSD(T)[c]		1.74		616.5	3.37					0.0
expt.		1.7450[d]	98.07[e] 102.0[f]	620.87[g]	3.365[g]			5.7 (7)[h]		0.0
				$\alpha^3\Sigma^+$						
MRCI/4Z	1739.11605	1.7429	65.6	680.3	3.6	0.0028	339.1	2.69 (2.7)	0.67	10370
MRCI+Q	1739.1684	1.740	54.0	680.7	3.7	0.0027	339.2			14091
RCCSD(T)/4Z	1739.19082	1.7402	52.9	678.2	4.3	0.0030	338.0			16123
C-RCCSD(T)+DKH2/C5Z	1753.96830	1.7360	56.1	679.1	4.0	0.0030	338.5	(2.64)	0.84	14733
MRCI[c]		1.73		676.9	1.98			(2.69)		8872
CCSD(T)[c]		1.73		689.8	5.04					14599
expt.[d]		1.7379		674.20	4.14					14580.5
				$A^1\Sigma^+$						
MRCI/4Z	1739.09327	1.7854	72.2	652.1	3.5	0.0026	325.4	2.36 (2.50)	0.70	15368
MRCI+Q	1739.15026	1.771	80.2	667.6	3.6	0.0026	332.9			18069
MRCI/5Z	1739.12192	1.7830	72.7	655.4	4.0	0.0027	326.6	2.24 (2.41)	0.75	15287
MRCI+Q	1739.1802	1.769	80.6	668.9	3.6	0.0027	333.6			17962
MRCI+DKH2/5Z	1753.37857	1.7894	66.3	636.7	3.2	0.0026	317.6	2.32 (2.55)	0.74	14479
MRCI+DKH2+Q/5Z	1753.4391	1.775	75.1	654.9	3.3	0.0026	326.7			16389
C-MRCI+DKH2/C5Z	1753.79858	1.7937	62.8	631.7	3.6	0.0027	315.0	2.39 (2.6)	0.79	14029
C-MRCI+DKH2+Q/C5Z	1753.90329	1.780	72.7	648.6	0.3	0.0029	325.6			15858
MRCI[c]		1.77		651.0	2.10			2.42		14371
EOM-CCSD[c]		1.76		667.1	4.93					18631
expt.[d]		1.7638								19301.4
				$b^3\Pi$						
MRCI/4Z	1739.09085	1.7508	69.1	660.6	3.6	0.0030	329.5	2.73 (3.10)	0.69	15899
MRCI+Q	1739.1406	1.742	73.1	665.5	3.5	0.0030	332.1			20189
RCCSD(T)/4Z	1739.17602	1.7601	84.5	646.7	3.4	0.0029	322.6	(2.55)	0.74	19371
C-RCCSD(T)+DKH2/C5Z	1753.95525	1.7524	81.2	648.1	3.2	0.0029	323.5	(2.53)	0.84	17596
MRCI[c]		1.75		639.0	1.73			2.77		11695
CCSD(T)[c]		1.75		651.5	2.96					17502
expt.		1.75558[i]		647.63[g]	3.458[g]					17543.2[g]
				$c^3\Delta$						
MRCI/4Z	1739.08796	1.8037	68.6	617.4	3.9	0.0027	307.8	3.23 (3.38)	0.70	16535
MRCI+Q	1739.1384	1.800	72.7	615.9	3.6	0.0027	307.2			20667
RCCSD(T)/4Z	1739.15873	1.8043	73.7	611.6	4.8	0.0031	304.2	(3.26)	0.75	23165
C-RCCSD(T)+DKH2/C5Z	1753.93776	1.7958	70.3	614.6	3.5	0.0026	306.4	(3.19)	0.84	21436
MRCI[c]		1.79		609.1	2.45			3.19		15244
CCSD(T)[c]		1.79		650.1	2.70					21374
expt.[d]										22639
				$B^1\Pi$						
MRCI/4Z	1739.07887	1.7529	61.6	657.5	3.8	0.0030	327.9	2.66 (2.96)	0.68	18530
MRCI+Q	1739.1292	1.745	66.0	662.8	4.8	0.0031	330.0			22682
MRCI+DKH2/5Z	1753.37326	1.7535	61.4	651.0	3.4	0.0030	324.9	2.62 (2.85)	0.74	15643
MRCI+DKH2+Q/5Z	1753.4267	1.746	66.4	655.4	3.9	0.0029	326.7			19115
MRCI[c]		1.74		638.8	0.55			2.65		14599
EOM-CCSD[c]		1.75		658.1	2.48					19438
expt.[d]		1.7539		643.73	3.66					20258.70
				$C^1\Delta$						
MRCI/4Z	1739.07592	1.8017	61.0	617.4	3.8	0.0030	308.5	2.98 (3.18)	0.69	19177
MRCI+Q	1739.1273	1.802	65.7	615.5	4.3	0.0030	307.6			23100
MRCI/5Z	1739.10410	1.8005	61.3	618.9	3.4	0.0028	308.7	2.90 (3.12)	0.76	19198
MRCI+Q	1739.1571	1.800	66.0	615.3	3.2	0.0030	307.0			23028
MRCI+DKH2/5Z	1753.3657	1.7926	58.0	621.0	3.7	0.0028	309.5	2.85 (3.00)	0.74	17297
MRCI+DKH2+Q	1753.4196	1.792	62.8	619.2	4.0	0.0031	308.6			20653

TABLE 6: Continued

method/basis set[a]	$-E$	r_e	D_e	ω_e	$\omega_e x_e$	α_e	ZPE	$\langle\mu\rangle$ (μ_{FF})[b]	Q_{Co}	T_e
C-MRCI+DKH2/C5Z	1753.78726	1.7927	55.3	622.4	2.4	0.0027	311.0	2.87 (3.03)	0.79	16512
C-MRCI+DKH2+Q	1753.8846	1.792	60.8	624.4	4.2	0.0029	311.1			19959
MRCI[c]		1.78		605.3	1.45			2.95		17825
EOM-CCSD[c]		1.79		660.6	2.37					23632

[a] +Q refers to the Davidson correction and DKH2 to second-order Douglas−Kroll−Hess scalar relativistic corrections. C- means that the Cu semicore $3s^23p^6$ electrons have been correlated. [b] $\langle\mu\rangle$ was calculated as an expectation value and μ_{FF} through the finite field method. [c] Ref 82. [d] Ref 60. [e] Ref 73, D_0 value. Chemiluminescence spectroscopy on the reaction $Cu^*(^2D_{5/2,3/2}) + ClF$. [f] Ref 49, D_0 value. Mass spectrometry on the reaction CuF + Ag = Cu + AgF. [g] Ref 66. [h] Ref 83. [i] Ref 63.

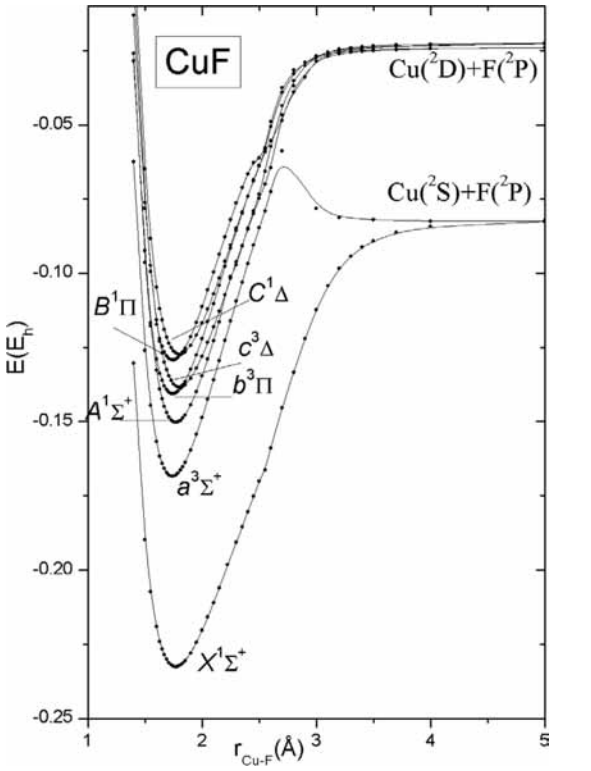

Figure 6. MRCI+Q potential energy curves of the CuF molecule. All energies are shifted by +1739.0 E_h.

cm^{-1} as compared to the experimental values of 1.7638 Å and 19301 cm^{-1}.[60] We believe that the dipole moment is calculated reliably, the suggested value being 2.50 D (Table 6).

The calculated values of the $B^1\Pi$ state are in relatively good agreement with the experiment,[60] our best results obtained at the MRCI+DKH2+Q/5Z level. Notice however that the MRCI+Q order of the two states $B^1\Pi$ and $c^3\Delta$ is not predicted correctly compared to the experimental ordering.

Finally, the $C^1\Delta$ is the highest calculated state of CuF; no experimental results are available for this state. It seems that the most consistent from the results shown in Table 6 are those obtained at the MRCI+DKH2+Q/5Z level. We suggest that r_e = 1.79 Å, D_e = 63kcal/mol, ω_e = 620 cm^{-1}, and $T_e(C^1\Delta-X^1\Sigma^+)$ = 21000−23000 cm^{-1}. The EOM-CCSD T_e value of ref 82 is 23632 cm^{-1}, in agreement with our MRCI+Q/4Z value. The dipole moment, $\mu_e \approx 3.1$ D, calculated more or less the same in all methods, should be very close to reality.

5. Synopsis and Remarks

For the fluorides FeF, CoF, NiF, and CuF, we have studied a total of 35 states employing multireference (MRCI) and coupled-cluster (RCCSD(T)) methods, in conjunction with basis sets of quadruple and quintuple quality. Using the quadruple basis set, we have also constructed full MRCI potential energy curves (PEC) for 29 states. It should be mentioned that despite the "chemical simplicity" of these systems, we encountered many technical difficulties in the PECs construction, particularly for the CuF system. In addition, although the calculation level is indeed high, we were not able to give definitive answers to certain questions raised in the literature.

TABLE 7: Recommended r_e (Å), D_e (kcal/mol), and μ_e (D) Values of the Ground States of the MF Series, M = Sc−Cu (Experimental Results in Parentheses)

species/X state	r_e	D_e[a]	μ_e[b]
ScF[c]/$^1\Sigma^+$	1.790	144	1.70
	(1.787)	(143.2 ± 3.2)	(1.72_2)
TiF[c]/$^4\Phi$	1.839	135	2.80
	(1.8311)	(136 ± 8)	(?)
VF[c]/$^5\Pi$	1.788	130	3.25
	(1.7758)	(?)	(?)
CrF[c]/$^6\Sigma^+$	1.785	110	4.25
	(1.7839)	(106.4 ± 3.5)	(?)
MnF[c]/$^7\Sigma^+$	1.840	108	2.80
	(1.8377)	(106.4 ± 1.8)	(?)
FeF/$^6\Delta$	1.783	109	2.50
	(1.78063)	(107 ± 5)	(?)
CoF/$^3\Phi$[d]	1.736	92 − 98[e]	4.60
	(1.7349)	(?)	(?)
NiF/$^2\Pi$[f]	1.736	103	5.20
	(1.73871)	(104.4 ± 1.4)	(?)
CuF/$^1\Sigma^+$	1.748	98	5.35
	(1.7450)	(98.07, 102.0)	(5.7_7)

[a] Experimental D_0 values. [b] RCCSD(T) values. [c] Ref 1. [d] X state formally of $^3\Phi$ symmetry, degenerate to the $^5\Delta$ and $^5\Phi$ states; see text. [e] See text. [f] X state formally of $^2\Pi$ symmetry, practically degenerate to the $^2\Sigma^+$ state; see text.

We report total energies, equilibrium bond lengths, binding energies, common spectroscopic constants, dipole moments, and energy separations. Most of our results are in good to excellent agreement with available experimental data. We summarize the salient results of the present work, including some results of our previous study on the earlier fluorides, ScF, TiF, VF, CrF, and MnF,[1] for a better understanding of these deceptively simple and interesting molecules.

All MF diatomics, M = Sc−Cu are highly ionic, with a Mulliken charge transfer of about 0.8 e^- from M to F. Because of the equilibrium ionic character of all MFs, the states studied can be understood as the corresponding atomic states of the M^+ cation in the field of $F^-(^1S)$.

Similarly to the earlier studied monofluorides,[1] PECs of the currently studied fluorides can be fitted perfectly to a Rittner-type potential[84]

$$V(r) = -\frac{1}{r} - \frac{A}{r^4} + Be^{-r/C}$$

where r is the intermolecular distance and A, B, and C are

adjustable parameters. Recall that the Rittner potential has been obtained from purely classical arguments to account for the dissociation energies of the ionic halides MeX, Me = Na, K,... and X = F, Cl,..., in the gas phase. Of course, the fitting fails beyond the ionic−covalent avoided crossing distance, namely, at around 3.5 Å.

Table 7 summarizes "recommended" ground-state r_e, D_e, and μ_e calculated values along with experimental ones for easy comparison. Observe, that as we move from Sc to Cu, the spin multiplicity increases, reaching a maximum of seven; then, it is reduced "regularly" to a singlet, reflecting the configuration of M^+. In addition, the range of bond lengths is narrow, the largest difference being 0.1 Å. Dissociation energies diminish, in general, monotonically from about 140 (ScF) to 100 kcal/mol (CuF). On the contrary, dipole moments rise as the atomic number increases, following a zigzag pattern from 1.7 (ScF) to 5.4 D (CuF).

We hope that this comprehensive study on the 3d transition-metal fluorides can be of some help to future experimental and theoretical studies on similar systems, diatomics or not.

References and Notes

(1) Koukounas, C.; Kardahakis, S.; Mavridis, A. *J. Chem. Phys.* **2004**, *120*, 11500.

(2) Kardahakis, S.; Koukounas, C.; Mavridis, A. *J. Chem. Phys.* **2005**, *122*, 054312.

(3) Harrison, J. F. *Chem. Rev.* **2000**, *100*, 679, and references therein.

(4) Bauschlicher, C. W., Jr. *Theor. Chim. Acta* **1995**, *92*, 183.

(5) (a) Balabanov, N.; Peterson, K. A. *J. Chem. Phys.* **2005**, *123*, 064107. (b) Balabanov, N.; Peterson, K. A. *J. Chem. Phys.* **2006**, *125*, 074110.

(6) (a) Dunning, T. H., Jr. *J. Chem. Phys.* **1989**, *90*, 1007. (b) Kendall, R. A.; Dunning, T. H., Jr.; Harrison, R. J. *J. Chem. Phys.* **1992**, *96*, 6796.

(7) (a) Werner, H.-J.; Knowles, P. J. *J. Chem. Phys.* **1988**, *89*, 5803. (b) Knowles, P. J.; Werner, H.-J. *Chem. Phys. Lett.* **1988**, *145*, 514.

(8) Werner, H.-J.; Knowles, P. J.; Lindh, R.; Manby, F. R.; Schütz, M. *MOLPRO*, version 2006.1; 2006.

(9) (a) Raghavachari, K.; Trucks, G. W.; Pople, J. A.; Head-Gordon, M. *Chem. Phys. Lett.* **1989**, *157*, 479. (b) Watts, J. D.; Gauss, J.; Bartlett, R. J. *J. Chem. Phys.* **1993**, *98*, 8718. (c) Knowles, P. J.; Hampel, C.; Werner, H.-J. *J. Chem. Phys.* **1993**, *99*, 5219. (d) Knowles, P. J.; Hampel, C.; Werner, H.-J. *J. Chem. Phys.* **2000**, *112*, 3106E.

(10) Douglas, M.; Kroll, N. M. *Ann. Phys. (N.Y.)* **1974**, *82*, 89.

(11) (a) Hess, B. A. *Phys. Rev. A: At., Mol., Opt. Phys.* **1985**, *32*, 756. (b) Hess, B. A. *Phys. Rev. A: At., Mol., Opt. Phys.* **1986**, *33*, 3742.

(12) (a) Jansen, H. B.; Ross, P. *Chem. Phys. Lett.* **1969**, *3*, 140. (b) Boys, S. F.; Bernardi, F. *Mol. Phys.* **1970**, *19*, 553.

(13) (a) Langhoff, S. R.; Davidson, E. R. *Int. J. Quantum Chem.* **1974**, *8*, 61. (b) Davidson, E. R.; Silver, D. W. *Chem. Phys. Lett.* **1977**, *52*, 403.

(14) Stanton, J. F.; Gauss, J.; Watts, J. D.; Nooijen, M.; Oliphant, N.; Perera, S. A.; Szalay, P. G.; Lauderdale, W. J.; Kucharski, S. A.; Gwaltney, S. R.; Beck, S.; Balkova, A.; Bernholdt, D. E.; Baeck, K. K.; Rozyczko, P.; Sekino, H.; Hober, C.; Bartlett, R. J. *ACES II*; Quantum Theory Project, University of Florida: Gainesvill, FL; Integral packages included are *VMOL* (Almlöf, J.; Taylor, P. R.), *VPROPS* (Taylor, P.); *ABACUS* (Helgaker, T.; Jensen, H. J. Aa.; Jørgensen, P.; Olsen, J.; Taylor, P. R.).

(15) (a) Blondel, C. *Phys. Scr.* **1995**, *58*, 31. (b) Linstrom, P. J., Mallard, W. G., Eds.; *NIST Chemistry WebBook, NIST Standard Reference Database Number 69*; National Institute of Standards and Technology: Gaithersburg, MD, 2005; http://webbook.nist.gov.

(16) (a) Pouilly, B.; Schamps, J.; Lumley, D. J. W.; Barrow, R. F. *J. Phys. B: At. Mol. Phys.* **1978**, *11*, 2281. (b) Pouilly, B.; Schamps, J.; Lumley, D. J. W.; Barrow, R. F. *J. Phys. B: At. Mol. Phys.* **1978**, *11*, 2289.

(17) Ram, R. S.; Bernath, P. F.; Davis, S. P. *J. Mol. Spectrosc.* **1996**, *179*, 282.

(18) (a) Allen, M. D.; Ziurys, L. M. *Astrophys. J.* **1996**, *470*, 1237. (b) Allen, M. D.; Ziurys, L. M. *J. Chem. Phys.* **1997**, *106*, 34–94.

(19) (a) Kermode, S. M.; Brown, J. M. *J. Mol. Spectrosc.* **2001**, *207*, 161. (b) Kermode, S. M.; Brown, J. M. *J. Mol. Spectrosc.* **2002**, *213*, 158.

(20) Gorokhov, L. N.; Ryzhov, M. Yu.; Khodeev, Yu. S. *Russ. J. Phys. Chem.* **1985**, *59*, 1761. as cited in ref 17.

(21) Bauschlicher, C. W., Jr. *Chem. Phys.* **1996**, *211*, 163.

(22) Tzeli, D.; Mavridis, A. *J. Chem. Phys.* **2003**, *118*, 4984.

(23) DeVore, T. C.; Van Zee, R. J.; Weltner, W., Jr. *Proc. Electrochem. Soc.* **1978**, *78−1*, 187.

(24) Adam, A. G.; Fraser, L. P.; Hamilton, W. D.; Steeves, M. *Chem. Phys. Lett.* **1944**, *230*, 82.

(25) (a) Ram, R. S.; Bernath, P. F.; Davis, S. P. *J. Mol. Spectrosc.* **1995**, *173*, 158. (b) Ram, R. S.; Bernath, P. F.; Davis, S. P. *J. Chem. Phys.* **1996**, *104*, 6949.

(26) Adam, A. G.; Hamilton, W. D. *J. Mol. Spectrosc.* **2001**, *206*, 139.

(27) Okabayashi, T.; Tanimoto, M. *J. Mol. Spectrosc.* **2003**, *221*, 149.

(28) Steimle, T. C.; Ma, T.; Adam, A. G.; Hamilton, W. D.; Merer, A. J. *J. Chem. Phys.* **2006**, *125*, 064302.

(29) Freindorf, M.; Marian, C. M.; Hess, B. A. *J. Chem. Phys.* **1993**, *99*, 1215.

(30) Krishnamurty, V. G. *Ind. J. Phys.* **1953**, *27*, 354.

(31) Pinchemel, B.; Lefebre, Y.; Schamps, J. *J. Mol. Spectrosc.* **1979**, *77*, 29.

(32) Pinchemel, Bernard, *J. Phys. B: At. Mol. Phys.* **1981**, *14*, 2569.

(33) Bai, J.; Hilborn, R. C. *Chem. Phys. Lett.* **1986**, *128*, 133.

(34) DeVore, T. C.; McQuaid, M.; Gole, J. L. *High Temp.* **1990**, *30*, 83.

(35) Dufour, C.; Carette, P.; Pinchemel, B. *J. Mol. Spectrosc.* **1991**, *148*, 303.

(36) Dufour, C.; Hikmet, I.; Pinchemel, B. *J. Mol. Spectrosc.* **1993**, *158*, 392.

(37) Dufour, C.; Hikmet, I.; Pinchemel, B. *J. Mol. Spectrosc.* **1994**, *165*, 398.

(38) Bouddou, A.; Dufour, C.; Pinchemel, B. *J. Mol. Spectrosc.* **1994**, *168*, 477.

(39) Dufour, C.; Pinchemel, B. *J. Mol. Spectrosc.* **1995**, *173*, 70.

(40) Focsa, C.; Dufour, C.; Pinchemel, B. *J. Mol. Spectrosc.* **1997**, *182*, 65.

(41) Chen, Y.; Jin, J.; Hu, C.; Yang, X.; Ma, X.; Chen, C. *J. Mol. Spectrosc.* **2000**, *203*, 37.

(42) Tanimoto, M.; Sakamaki, T.; Okabayashi, T. *J. Mol. Spectrosc.* **2001**, *207*, 66.

(43) Jin, J.; Ran, Q.; Yang, X.; Chen, Y.; Chen, C. *J. Mol. Spectrosc.* **2001**, *208*, 18.

(44) Jin, J.; Ran, Q.; Yang, X.; Chen, Y.; Chen, C. *J. Phys. Chem. A* **2001**, *105*, 11177.

(45) Kouti, Y.; Hirao, T.; Dufour, C.; Boulezhar, A.; Pinchemel, B.; Bernath, P. F. *J. Mol. Spectrosc.* **2002**, *214*, 152.

(46) Pinchemel, B.; Hirao, T.; Bernath, P. F. *J. Mol. Spectrosc.* **2002**, *215*, 262.

(47) Benomier, M.; Van Groenendael, A.; Pinchemel, B.; Hirao, T.; Bernath, P. F. *J. Mol. Spectrosc.* **2005**, *233*, 244.

(48) *IVTANTHERMO*, Database on ThermodynamicPropeties of Individual Substances; CRC Press: Boca Raton, FL, 2005.

(49) Hildenbrand, D. L.; Lau, K. H. *J. Phys. Chem. A* **2006**, *110*, 11886.

(50) Zou, W.; Liu, W. *J. Chem. Phys.* **2006**, *124*, 154312.

(51) Roos, B. O.; Lindh, R.; Malmqvist, P.-Å.; Veryazov, V.; Widmark, P.-O. *J. Phys. Chem. A* **2005**, *109*, 6575.

(52) Mulliken, R. S. *Phys. Rev.* **1925**, *26*, 1.

(53) Ritschl, R. *Z. Physik.* **1927**, *42*, 172.

(54) Woods, L. H. *Phys. Rev.* **1943**, *64*, 259.

(55) Kent, R. A.; McDonald, J. D.; Margrave, J. L. *J. Phys. Chem.* **1966**, *70*, 874.

(56) Hildenbrand, D. L. *J. Chem. Phys.* **1968**, *48*, 2457.

(57) Steele, R. E.; Broida, H. P. *J. Chem. Phys.* **1978**, *69*, 2300.

(58) Schwenz, R. W.; Parson, J. M. *J. Chem. Phys.* **1980**, *73*, 259.

(59) Lee, E. P. F.; Potts, A. W. *Chem. Phys. Lett.* **1980**, *76*, 532.

(60) Ahmed, F.; Barrow, R. F.; Chojnicki, A. H.; Dufour, C.; Schamps, J. *J. Phys. B: At. Mol. Phys.* **1982**, *15*, 3801.

(61) Steimle, T. C.; Brazier, C. R.; Brown, J. M. *J. Mol. Spectrosc.* **1982**, *91*, 137.

(62) Brazier, C. R.; Brown, J. M.; Steimle, T. C. *J. Mol. Spectrosc.* **1983**, *97*, 449.

(63) Brazier, C. R.; Brown, J. M.; Purnell, M. R. *J. Mol. Spectrosc.* **1983**, *99*, 279.

(64) Steimle, T. C.; Brazier, C. R.; Brown, J. M. *J. Mol. Spectrosc.* **1985**, *110*, 39.

(65) Delaval, J. M.; Lefebre, Y.; Bocket, H.; Bernage, P.; Niay, P. *Chem. Phys.* **1987**, *111*, 129.

(66) Baltayan, P.; Hartmann, F.; Pebay-Peyroula, J. C.; Sadeghi, N. *Chem. Phys.* **1988**, *120*, 123.

(67) Delaval, J. M.; Schamps, J.; Dufour, C. *J. Mol. Spectrosc.* **1989**, *137*, 268.

(68) Parson, J. M.; Fang, C. C. *J. Chem. Phys.* **1990**, *92*, 4823.

(69) Fang, C. C.; Parson, J. M. *J. Chem. Phys.* **1991**, *95*, 6413.

(70) Jakob, P.; Sugawara, K.; Wanner, J. *J. Mol. Spectrosc.* **1993**, *160*, 596.

(71) Jakob, P.; Sugawara, K.; Wanner, J.; Bath, A.; Tiemann, E. *Can. J. Phys.* **1994**, *72*, 1087.

(72) Okabayashi, E.; Yamazaki, E.; Honda, T.; Tanimoto, M. *J. Mol. Spectrosc.* **2001**, *209*, 66.

(73) Sadeghi, N.; Kowalczyk, P.; Setser, D. W. *Phys. Chem. Chem. Phys.* **2003**, *5*, 3443.
(74) Dufour, C.; Schamps, J.; Barrow, R. F. *J. Phys. B: At. Mol. Phys.* **1982**, *15*, 3819.
(75) DeLaval, J. M.; Schamps, *J. Chem. Phys.* **1985**, *100*, 21.
(76) Ramirez Solis, A; Daudey, J. P. *Chem. Phys.* **1989**, *134*, 111.
(77) Kölmel, C.; Ahlrichs, R. *J. Phys. Chem.* **1990**, *94*, 5536.
(78) Schamps, J.; Delaval, J. M.; Faucher, O. *Chem. Phys.* **1990**, *145*, 101.
(79) Ramirez Solis, A. *Phys. Rev. A* **1993**, *47*, 1510.
(80) Hrušák, J.; Ten-no, S.; Iwata, S. *J. Chem. Phys.* **1997**, *106*, 7185.
(81) Iliaš, M.; Furdik, P.; Urban, M. *J. Phys. Chem. A* **1998**, *102*, 5263.
(82) Guinchemerre, M.; Chambaud, G.; Stoll, H. *Chem. Phys.* **2002**, *280*, 71.
(83) Huber, K. P.; Herzberg, G. H. Molecular Spectra and Molecular Structure, Vol. IV. *Constants of Diatomic Molecules*; Van Nostrand Reinhold: New York, 1979.
(84) Rittner, E. S. *J. Chem. Phys.* **1951**, *19*, 1030.

JP805034W